In vitro evidence against productive SARS-CoV-2 infection of human testicular cells: Bystander effects of infection mediate testicular injury.

Stefanos Giannakopoulos[1], Daniel P Strange[2], Boonyanudh Jiyarom[2], Omar Abdelaal[3], Aaron W Bradshaw[3,4], Vivek R Nerurkar[2], Monika A Ward[5], Jackson Bakse[5], Jonathan Yap[6], Selena Vanapruks[6], William Boisvert[6], Michelle D Tallquist[1], Cecilia Shikuma[2], Hooman Sadri-Ardekani[3,4], Philip Clapp[3], Sean Murphy[3], Saguna Verma[1,2#].

[1]Department of Cell and Molecular Biology, John A. Burns School of Medicine, University of Hawaii at Manoa, Honolulu, Hawaii, USA

[2]Department of Tropical Medicine, Medical Microbiology, and Pharmacology, John A. Burns School of Medicine, University of Hawaii at Manoa, Honolulu, Hawaii, USA

[3]Wake Forest Institute for Regenerative Medicine, Wake Forest School of Medicine, Winston-Salem, North Carolina

[4]Department of Urology, Wake Forest School of Medicine, Winston-Salem, North Carolina

[5]Institute for Biogenesis Research, John A Burns School of Medicine, University of Hawaii at Manoa, Honolulu, Hawaii, USA

[6]Center for Cardiovascular Research, John A. Burns School of Medicine, University of Hawaii at Manoa, Honolulu, Hawaii, USA

Running Title: SARS-CoV-2 infection-derived mediators mediate testicular injury

#Corresponding author: Saguna Verma

E-mail: saguna@hawaii.edu

Abstract

The hallmark of severe COVID-19 involves systemic cytokine storm and multi-organ failure including testicular injury and germ cell depletion. The ACE2 receptor is also expressed in the resident testicular cells however, SARS-CoV-2 infection and mechanisms of testicular injury are not fully understood. The testicular injury can likely result either from direct virus infection of resident cells or by exposure to systemic inflammatory mediators or virus antigens. We here characterized SARS-CoV-2 infection in different human testicular 2D and 3D models including primary Sertoli cells, Leydig cells, mixed seminiferous tubule cells (STC), and 3D human testicular organoids (HTO). Data shows that SARS-CoV-2 does not establish a productive infection in any testicular cell types. However, exposure of STC and HTO to inflammatory supernatant from infected airway epithelial cells and COVID-19 plasma depicted a significant decrease in cell viability and death of undifferentiated spermatogonia. Further, exposure to only SARS-CoV-2 envelope protein, but not Spike or nucleocapsid proteins led to cytopathic effects on testicular cells that was dependent on the TLR2 receptor. A similar trend was observed in the K18h-ACE2 mouse model which revealed gross pathology in the absence of virus replication in the testis. Collectively, data strongly indicates that the testicular injury is not due to direct infection of SARS-CoV-2 but more likely an indirect effect of exposure to systemic inflammation or SARS-CoV-2 antigens. Data also provide novel insights into the mechanism of testicular injury and could explain the clinical manifestation of testicular symptoms associated with severe COVID-19.

Introduction:

SARS coronavirus 2 (SARS-CoV-2), a positive-sense RNA virus, emerged in China in December 2019 and has since evolved into different variants and spread across the globe causing mild to severe coronavirus disease known as COVID-19. SARS-CoV-2 infects susceptible human cells by binding to Angiotensin-Converting Enzyme 2 (ACE2) and causes a range of clinical symptoms, which can progress to severe COVID-19 based on vaccination status and co-morbidities (1, 2). In addition to the acute lung injury with diffuse alveolar damage, other hallmarks of severe COVID-19 include multi-organ injury including vascular inflammation, cardiac complications, and kidney failure (3, 4). Epidemiological studies suggest that males irrespective of age and co-morbid conditions are disproportionately affected and present a higher case-to-fatality ratio than females (5).

Recent pathological and clinical findings provide evidence that a large percentage of males with COVID-19 report mild orchitis (inflammation of the testis associated with pain and discomfort) as one of the symptoms (6). Further, postmortem analysis of testis from COVID-19 patients display signs of mild to severe testicular pathology, including testicular swelling, tubular injury, germ cell and LC depletion, and leukocyte infiltration in the interstitium (5, 7, 8). In addition, alterations in the male fertility parameters like reduced sperm count, reduced testosterone levels, and dysregulated ratio of testosterone to LH (T/LH) have been reported in COVID-19 patients (9, 10). However, while the virus has not been detected in the semen in several studies (11, 12), one study reported the presence of low levels of SARS-CoV-2 RNA in the semen of 4/15 of patients at the acute stage of infection and in 2/23 patients who were recovering from COVID-19 (13). Although

the presence of viral RNA is not direct evidence of productive infection of SARS-CoV-2 in the testis, and the ability of the virus to gain access to the testis may be a rare event, these data do suggest that testicular injury is one of the complications of COVID-19.

SARS-CoV-2 viral replication and pathogenesis in extra-pulmonary organs are currently not well understood. Emerging data demonstrate the presence of low-level viral RNA and virus-like particles (VLPs) in many organs like the heart, kidney, testis, intestine, and brain (8, 14–16). SARS-CoV-2 VLPs, comprised of all major structural proteins including Spike (S), Nucleocapsid (N), Membrane (M), and Envelope (E), are abundantly secreted by the infected cells and can enter cells just like SARS-CoV-2 infectious virions (17). In addition, more recent studies detected SARS-CoV-2 proteins like S, N, and open reading frame 8 (ORF8) in the plasma of infected individuals illustrating antigenemia as one of the hallmarks of SARS-CoV-2 infection (18, 19). Exposure of both S and N proteins induced pro-inflammatory cytokines including interleukin 6 (IL-6) and tumor necrosis factor-alpha (TNF-α) in human macrophages (20, 21). It is not known if the E protein is also secreted in the bloodstream, but it is shown to form cation channels in the lipid bilayer and trigger the hyperinflammatory response in human macrophages and mice (22). While specific mechanisms by which SARS-CoV-2 cause testicular injury are still being characterized, the cytokine storm is considered to be the main driving factor of damage to organs other than lungs in severe COVID-19 patients (23). The testicular inflammation can likely result either from direct virus infection of target cells or by exposure to systemic inflammatory mediators or virus antigens.

In humans, testis show a very high level of constitutive gene expression of angiotensin converting enzyme 2 (ACE2) that regulates testosterone production and interstitial fluid volume via modulating conversion of Angiotensin II to Angiotensin I (24, 25). The single-cell RNA-sequencing datasets from human testes revealed high expression of ACE2 in undifferentiated spermatogonia including spermatogonia stem cells (SSC), Leydig (LC), and Sertoli cells (SC) (26). However, although transmembrane serine protease 2 (TMPRSS2) is expressed in most of the cell types in the body, there are conflicting reports on its expression levels and co-expression with ACE2 in different testicular cells (27, 28). The presence of ACE2 receptor in multiple resident cells hypothetically makes the testes a potential target for SARS-CoV-2 infection or endocytosis of VLPs. Alternatively, systemic cytokine storm may induce bystander testicular inflammation, thus explaining the orchitis symptom observed in COVID-19 patients. Therefore, the question remains whether the gonadal injury is the direct or indirect consequence of virus infection in the testes.

Here, using both 2D and 3D human multicellular testicular cell culture models, we show that SARS-CoV-2 can enter testicular cells, but cannot establish productive virus infection. Exposure of testicular cells with inflammatory media from SARS-CoV-2 infected human airway epithelial cells led to apoptotic death of undifferentiated spermatogonia. Further, only exposure to SARS-CoV-2 E protein but not S1 and N protein induced a pro-inflammatory response that correlated with severe cytotoxicity. We also carefully examined and validated the bystander effect of SARS-CoV-2 infection on testicular injury using K18-hACE2 mice. Our data collectively provide the first evidence that the testicular

116 injury is not due to direct infection of SARS-CoV-2 but more likely an indirect effect of
117 exposure to systemic inflammation or SARS-CoV-2 antigens.
118
119 **Materials and Methods**
120 **Cells, Testicular Organoids, and Virus infection:**
121 Primary human SC and LC were obtained from iXCells Biotechnologies and ScienCell
122 Research Laboratories, respectively. Low passage SC and LC were cultured in DMEM/F-
123 12 and Leydig Cell Medium as described previously (29). The human testicular organoids
124 (HTO) consisting of primary SC, LC, peritubular myoid cells (PMC), and undifferentiated
125 spermatogonia (SSC) were generated from adult human testicular tissue procured
126 through the National Disease Research Interchange (NDRI) and cultured in ultralow-
127 attachment 96-well round-bottom plates as described by us previously (30, 31). For mixed
128 seminiferous tubule cells (STC) culture, seminiferous tubules from adult testes were
129 digested to isolate mixed cell populations of SC, PMC, and SSC as described previously
130 (32). SARS-CoV-2 USA-WA1/2020 strain was obtained from BEI Resources, propagated
131 once in Vero E6 cells, and used for all in vitro experiments. Cells cultured in 6-, 24-, or
132 96-well plates were infected with SARS-CoV-2 at MOI 1 or 10 and incubated for 1.5 hrs
133 at 37% and 5% CO2. HTO were infected using 10^4 PFU SARS-CoV-2. All SARS-CoV-2
134 manipulations were performed in the dedicated BSL3 facility at the John A. Burns School
135 of Medicine.
136
137 **Virus quantitation:**

SARS-CoV-2 titers in cell culture supernatants were measured by plaque assay using Vero E6 cells and expressed as PFU per mL of supernatant (33). Intracellular viral genome copies were measured in the RNA extracted from cell lysates and tissue homogenates at different time points post-infection by qRT-PCR. Forward (nCoV_IP4-14059Fw: GGTAACTGGTATGATTTC G) and reverse (nCoV_IP4-14146Rv: CTGGTCAAGGTTAATATAGG) primers and probe (nCoV_IP4-14084Probe(+): TCATACAAACCACGCCAGG [5']Fam [3']BHQ-1) were used specific for SARS-CoV-2 RNA-dependent RNA polymerase gene region and expressed as genome copies per µg of RNA (34).

Exposure of testicular cells to inflammatory media, COVID-19 plasma, and SARS-CoV-2 proteins exposure:

Human airway epithelial cells (HAE) grown on the inserts were infected with SARS-CoV-2 at MOI 1 as described by others (35). Media was collected from the basal and the apical side of inserts at different time points after infection. The basal side supernatant was treated with ultraviolet light (UV) for 12 min to inactivate infectious virions. Different testicular models were exposed to UV-inactivated HAE supernatant (1:1 ratio with cell culture media). SC and STC cultures were also exposed to SARS-CoV-2 E, N or S1 proteins at 1 or 4 ng/µL concentration. Plasma from 5 RT-PCR+ COVID-19 patients collected during the symptomatic phase (days 4-6 of symptoms) under the UH IRB# 2020-00367 and age-matched healthy controls were used in this study. STC and HTOs were exposed to plasma (1:5 ratio with cell media) and cell viability and TUNEL staining assays were conducted after 24 hrs of exposure. The E protein was also incubated with 1X

proteinase K for 3 hrs before exposing to SC. In some experiments, E and S1 exposure were conducted in the presence or absence of neutralizing antibodies against toll-like receptor 2 and 4 (TLR2 and TLR4) antibodies (ThermoFisher Scientific Cat. # MA5-16200 and Cat # MA180122 at 1:250 and 1:500 concentration respectively).

RT-PCR analysis:

Total RNA was extracted from mock- and SARS-CoV-2-infected SC, LC, STC, and HTO lysates using RNeasy mini kit (Qiagen) and synthesized into cDNA, and change in mRNA transcripts of inflammatory genes was measured by qPCR, as described previously (36). Specific primer sequences are either previously described (29, 37) or shown in Table 1. The housekeeping gene *GAPDH* was used to normalize fold change values of antiviral genes, with respective controls used as a reference control.

Cell Viability:

Cell viability of different 2D cultures at different time points of infection or exposure to virus proteins or HAE supernatant was determined using the CellTiter 96 AQueous One Solution cell proliferation assay (G3582; Promega), while HTO viability was determined by the CellTiter-Glo 3D cell viability assay (Promega G9681; Promega) as described previously (29).

Enzyme-Linked Immunosorbent Assays:

All commercially available ELISA kits were purchased from Invitrogen Thermo Fisher Scientific and the assays were performed according to the manufacturer's instructions.

The kits used were IL-6 Human Instant ELISA Kit (Cat. # BMS213INST), IL-1β Human Instant ELISA Kit (Cat. # BMS224INST), and TNF-alpha human Instant ELISA Kit (Cat. # BMS223INST). All samples including HAE supernatant at different time points and plasma from COVID-19 patients were run in triplicate and levels were expressed as pg/mL media or plasma.

Immunofluorescence and TUNEL assay:

Mock and infected LC, SC, or STC grown on glass coverslips were fixed with 4% PFA, permeabilized with 0.1% Triton X-100 in PBS, and blocked with 5% bovine serum albumin in PBS. Cells were then incubated with primary antibodies against anti-Spike (GeneTex, GTX632604 at 1:500 dilution), followed by fluorophore-conjugated secondary antibody (Invitrogen Alexa Fluor 488-conjugated sheep anti-rabbit, 1:5000 dilution), and examined using an Axiocam MR camera mounted on a Zeiss Axiovert 200 microscope. TUNEL assay was performed using the Promega DeadEnd^{TM} Fluorometric TUNEL System according to the manufacturer's instructions. Undifferentiated spermatogonia were also stained for the well-established cell-specific marker, ubiquitin carboxyl-terminal esterase L1 (UCHL1) (29) using rabbit anti-human UCHL1 (Sigma, HPA005993 at 1:1,000 dilution). The secondary antibody was Alexa Fluor 594-conjugated goat anti-rabbit (Invitrogen; 1:5000 dilution).

Infection of *K18-hACE2* mice

B6.Cg-Tg(K18-ACE2)2Prlmn/J (*K18-hACE2*) mice (#034860) were obtained from the Jackson Laboratory. All mouse experiments were performed according to the animal

experimental guidelines issued and approved by Institutional Animal Care and Use Committee of the University of Hawaii at Manoa. All mouse infection experiments were conducted using SARS-CoV-2 USA-HI-B.1.429 isolated from a local COVID-19 patient in 2020 that is very similar to the SARS-CoV-2 CoV/USA-WA1/2020 (38) at the dedicated ABSL2/3 facility at the UH. Eight to twelve weeks old *K18-hACE2* mice were inoculated with $2x10^4$ PFU SARS-CoV-2 via the intranasal route and observed daily to record body weights and clinical symptoms and were sacrificed when weight loss greater or equal to 20% was observed. The lung, heart, and testis tissues were harvested in a separate set of experiments at 3, 5, and 8 days post infection (dpi) and were either flash-frozen or fixed in 4% PFA to determine virus genome copies and histopathological changes respectively. RNA was extracted from frozen tissues as described previously (39) and virus RNA and expression of different host genes were measured by RT-PCR. Testes were also fixed in Bouin overnight, and then stored in 70% ethanol prior to embedding in paraffin wax, sectioning at 5 µm, and staining with Periodic acid Schiff and hematoxylin (PASH) to identify histopathological changes.

Statistical Analysis:

All data were analyzed with GraphPad Prism 9.3.1 software. Statistically significant differences between different groups were determined using unpaired t-tests. SARS-CoV-2 titers and viability data are reported as means +/- standard error of the mean (SEM) from at least three or more independent experiments. Gene expression (mRNA fold change) and ELISA data are reported as means +/- standard errors of the means

(SEM) from ≥3 independent experiments. A *p-value* of <0.05 was considered statistically significant for all analyses.

Results:

Human testicular cells do not support productive SARS-CoV-2 infection. We, and others, have previously shown that human testicular cells like LC and SC express ACE2 (40). Therefore, we first determined the infection kinetics of SARS-CoV-2 in different testicular cell models including primary human SC and LC, 2D culture of mixed STC and 3D HTOs. Low levels of viral RNA in the range of log 2-3 genome copies were detected in all cell models, but the virus copies did not increase between 24 and 96 hrs post-infection (hpi, Fig. 1A). Virus titers measured in the supernatant by plaque assay did not show the presence of infectious virions in any cell types at any time point (Fig. 1B). These data suggest that productive replication of SARS-CoV-2 did not occur in these human testicular cell models. Infection of SC and LC at higher MOI 10 also did not show any SARS-CoV-2 released in the supernatant over 96 hours (Fig. S1A-B). In addition, we were not able to detect the SARS-CoV-2 spike protein using immunofluorescence assay in infected SC and LC (Fig. 1C), further demonstrating the lack of SARS-CoV-2 replication in these primary cell cultures.

Since exogenous serine proteases have been shown to facilitate SARS-CoV-2 entry and replication in other low TRMPSS2 expressing cells (41), we next assessed if TRMPSS2 is expressed in LC and SC and if the presence of exogenous serine protease activity would make testicular cells susceptible to infection. We observed that there was minimal

to no TMPRSS2 staining in these cells (Fig. S1C). Assuming that this could be a factor explaining non-productive SARS-CoV-2 infection in these cell types, we analyzed virus replication in the presence of exogenous serine protease. SARS-CoV-2 infection of SC pre-incubated with 5 µg/mL trypsin, a serine protease, which at this concentration does not interfere with cell attachment and has been used by others to enhance SARS-CoV-2 entry in other cell types (42), also did not result in increased intracellular virus RNA (data not shown) or infectious virions in the supernatant (Fig. 1D). To further evaluate if SARS-CoV-2 entry alone can activate an inflammatory response, we measured the mRNA levels of key cytokines associated with COVID-19 in SC, LC, and HTO at 48 hpi. Consistently, gene expression of inflammatory cytokines including *IL6, TNFA,* and interferon beta 1 *(IFNB1)* was not altered in any of these testicular cell types (Fig. 1E). Collectively, our data strongly suggest that even though SARS-CoV-2 RNA is detected in testicular tissue from COVID-19 patients, it does not establish a productive infection in resident human testicular cells.

SARS-CoV-2 infection of human airway epithelial cells is associated with loss of air-liquid barrier integrity and production of inflammatory cytokines.

Several clinical studies have linked SARS-CoV-2-associated cytokine storm with injury to the kidney, heart, and brain (43–49). Therefore, we next tested if the testicular damage was an indirect effect of the inflammatory mediators derived from SARS-CoV-2 infection of other cell types. To begin the evaluation of the bystander effect, we first infected well differentiated 2D cultures of human airway epithelial cells (HAE) grown on transwell inserts at MOI 1 and measured infectious virions released both on the apical and basal

sides of the inserts. The plaque assay demonstrated a significant increase in the virus titers at 2 days post-infection (dpi) that peaked at day 3 and subsequently declined by >2 logs by 8 dpi (Fig. 2A). A similar trend was observed in intracellular virus genome copies, with peak virus replication at 4 dpi (Fig. 2B). Further, SARS-CoV-2 infection also compromised the integrity of the air-liquid barrier (Fig. 2C). The transepithelial electrical resistance (TEER) readings showed a decline starting at 3 dpi with significantly lower values at 5 and 6 dpi, suggesting a loss in the barrier integrity most likely a result of virus-induced CPE. Peak virus titers also correlated with significant induction of key inflammatory cytokine genes like *TNFA* and *IL6,* and antiviral genes including interferon-induced protein with tetratricopeptide repeats one (*IFIT1*) at 4 dpi (Fig. 2D).

The production of key cytokines in the HAE supernatant was further confirmed and compared to plasma from COVID-19 patients during the acute stage of the disease (4-6 days of symptom onset) using ELISA. While there was no difference in the levels of IL-1β, TNF-α, and IL-6 in mock and infected HAE supernatant at 1 dpi (data not shown), as seen in Fig. 3A-C, their levels were significantly higher in the infected supernatant at 4 dpi that correlated with peak virus titers. Further, interestingly, the levels of these cytokines were comparable to the levels seen in the plasma of COVID-19 patients (Fig. 3A-C). Collectively, this data shows that supernatant from SARS-CoV-2 infected HAE mimics the profile of select cytokines observed in COVID-19 patients and can be used to evaluate the indirect effect of infection on 2D and 3D human testicular models.

297 **SARS-CoV-2 infection-derived inflammatory mediators cause indirect cytotoxicity**
298 **on primary human testicular cells**

299 To determine the cytotoxic effects of SARS-CoV-2 infection-derived inflammatory
300 mediators on testicular cells, we exposed STC to UV-inactivated supernatant from HAE
301 and COVID-19 plasma and measured the cell viability. As seen in Fig. 3D, at 24hrs post-
302 exposure, the cell viability of the STC exposed to infected HAE supernatant declined by
303 approximately 30%. In contrast, the viability of cells exposed to supernatant from mock-
304 infected HAE cells was comparable to untreated cells. Similarly, an almost 50% decrease
305 in the viability of STC and HTO was observed when exposed to COVID-19 plasma as
306 compared to healthy control plasma (Fig. 3E). To further understand if cell death following
307 exposure to inflammatory plasma also triggers cytotoxic cytokines, we measured mRNA
308 levels of *IL6, IL1B,* and *TNFA* genes. There was a significant increase in the transcripts
309 of these cytokines as well as Bcl-2 associated protein X (*BAX)*, a pro-apoptotic gene, in
310 HTO exposed to COVID-19 plasma (Fig. 3G). Interestingly, SC alone exposed to infected
311 HAE supernatant did not exhibit any significant change in cell viability at 24 hours post-
312 exposure (Fig. 3F). We also did not observe a similar induction of cytokines and *BAX* in
313 SC following exposure to HAE supernatant (Fig. 3H), suggesting that the cell death seen
314 in our mixed 2D and 3D cultures was most likely of the delicate germ cells.

315

316 To further validate that undifferentiated spermatogonia are more susceptible to cell death,
317 we conducted a TUNEL assay on STC exposed to both UV-inactivated HAE supernatant
318 and COVID-19 plasma for 24 hours. As seen in Fig. 4A, very few TUNEL-positive cells
319 were detected in STC that were untreated or treated with mock HAE supernatant.

However, TUNEL positive cells increased significantly from 2% in mock to 10% in STC treated with infected supernatant for 24 hrs (Fig. 4B). Similarly, TUNEL positive cells increased from 6% in healthy control plasma-treated cells to 20% in COVID-19 plasma-treated STC (Fig. 4A-B). The cells were also co-stained for UCHL1, a well-established undifferentiated spermatogonia marker, and merged pictures in Fig. 4C show that UCHL1 positive cells were also TUNEL positive (yellow) in STC exposed to infected supernatant from HAE cells. However, in STC exposed to COVID-19 plasma, we observed apoptotic cell death in both UCHL1 positive and UCHL1 negative cells (white arrows). These findings suggest that mediators derived from SARS-CoV-2 infection in the HAE supernatant and COVID-19 plasma can cause an inflammatory response in testicular cells and apoptotic cell death.

SARS-CoV-2 envelope protein causes severe damage in testicular cells

Virus-induced bystander cell death can be because of both, the inflammatory cytokines or viral proteins secreted by infected cells in the bloodstream, as shown in other viruses like Dengue and Ebola (50–52). As a result, we investigated whether SARS-CoV-2 S1, N, and E proteins can cause cytopathic effects in various testicular cells. The SC were exposed to recombinant SARS-CoV-2 E, N, and S1 at different concentrations (0.25, 0.5, 1 and 4ng/µL) and cell viability was quantified at 24hrs post-exposure. While the S1 and N proteins did not affect the cell viability, we observed a significant reduction in the viability after exposure to the E protein in a dose-dependent manner with the most severe cell death seen in cells treated with 4 ng of E (Fig. 5A). Further, to examine whether SC cytotoxicity was specific to envelope protein, we pre-incubated envelope protein with

proteinase K. SC death was reversed when E protein was inactivated with proteinase K indicating that E alone can cause SC death (Fig. 5A). We then treated STC with E and S1 at concentrations 1 and 4 ng/well and measured cell death at 4 and 24hrs post-exposure and demonstrated a 30-40% decrease in cell viability only in E-treated STCs (Fig. 5B). Similarly, E protein treated HTO showed a 40% reduction in cell viability at 24hrs post-exposure (Fig. 5C). To further validate if the cell death associated with the E protein is associated with cytokine induction, we measured the levels of cytotoxic cytokines like IL-6, TNF-α, and IL-1β in the supernatant of STC exposed to E and S1 proteins using ELISA. As seen in Fig. 5D-F, these cytokines were either absent or detected at very low levels in mock and S1-treated STC. However, their levels were significantly increased by E protein as early as 4hrs post-exposure and further increased at 24hrs post-exposure. The induction of IL-6, TNF-α, and IL-1β was also validated at the transcript level (Fig. 5G), and the fold-increase of these cytokines at 24 hrs post-exposure to E protein correlated well with the ELISA data. Moreover, we also observed a > 20-fold increase in the transcripts of the pro-apoptotic gene BAX (Fig. 5G).

Secretory virus proteins can activate inflammatory pathways following binding to cell surface receptors including TLR2 and/or 4 (50, 53). Therefore, to examine the involvement of TLR2 and 4 in the cytopathic effects associated with E, we exposed STC to E protein in the presence or absence of neutralizing antibodies against TLR2 and TLR4. As seen in Fig. 5H, while the presence of neutralizing TLR4 antibody did not affect the cell viability outcome, there was a nearly complete reversal in the cell death caused by E protein in the presence of anti-TLR2. Similarly, there was a reversal in the cell death

366 induced by E protein in SC in the presence of anti-TLR2 (data not shown) suggesting that
367 the downstream response of the E protein involves activation of the TLR2 receptor
368 signaling.
369
370 To further determine if the cellular uptake of E protein is required for the cytopathic effects,
371 we visualized STC exposed to E and S1 proteins conjugated with fluorophore AF488
372 using confocal microscopy. As seen in Fig. 6A-B, E protein was internalized efficiently by
373 STC after 12hrs of exposure and was detected mainly in the cytoplasm of these cells
374 (white arrows). The intensity of the staining for Phalloidin, a marker for actin filaments,
375 was significantly reduced in E protein-treated STC (Fig. 6C-D) indicating that the
376 cytoskeleton was degraded. Further, the DNA (blue arrows) was ejected from the nuclei
377 of E protein-positive cells (Fig. 6A), suggesting significant disruption of STC homeostasis.
378 In contrast, it appeared that the internalization of S1 protein was significantly lower than
379 E protein and did not lead to disruption of the cytoskeleton or overall morphology (Fig.
380 6C-D). Collectively, these data firmly establish that the SARS-CoV-2 E protein can be
381 efficiently internalized by testicular cells and causes severe cell death that is dependent
382 on TLR2 and is accompanied by an increase in the production of inflammatory cytokines.
383
384 **SARS CoV-2 infection of K18-hACE2 mice leads to testicular inflammation and**
385 **injury.**
386 To characterize the effect of SARS-CoV-2 infection on the testis in vivo, we utilized the
387 transgenic K18-hACE2 mouse model that expresses high levels of human ACE2 in the
388 lung, low levels in the brain, and none in other epithelial cells like GI and liver (54).

Compared to other animal models like hamsters, ferrets, and primates, the K18-hACE2 mouse model best mimics different aspects of COVID-19 including severe disease, systemic cytokine storm, and tissue injury (55–57). Since testicular injury is most commonly seen in moderate to severe COVID-19 patients, these mice are best suited for studying the indirect effects of SARS-CoV-2 infection on the testis. Intranasal inoculation of K18-hACE2 mice with $2x10^4$ PFU of SARS-CoV-2 led to almost 70-80% mortality (Fig. 7A) that replicated outcomes of similar studies (58, 59). Virus genome copies in the lungs peaked at 3 dpi and remained high at 5 dpi (Fig. 7B**)** and were almost cleared by 8 dpi. However, virus mRNA was either found at very low levels in the heart in 50% of mice (Fig. 7B) or not detected at all in other peripheral tissues like the kidney and spleen (data not shown). Interestingly, we also did not detect virus RNA in any of the testes at any time point (Fig. 7B). Further, plaque assay of the tissue lysates demonstrated high virus titers present only in the lung lysates at 3 and 5 dpi but not in heart and testis lysates **(Fig. 7C).** We next assessed if inflammation markers are induced by the virus in the testes independent of active virus replication. As expected *IL6* and *TNFA* were upregulated in the lungs and correlated with viral titers. Interestingly, despite no viral RNA, we found that the transcripts of these inflammatory cytokines were significantly increased in the testes at 5 and 8 dpi.

To further assess if there is an indirect effect of SARS-CoV-2 infection on the testes, we conducted a histopathological assessment of PAS-H-stained sections of the testes. The uninfected control males had normal testis and tubular organization (Fig. 7E, i-ii). Seminiferous tubules were well-developed and tightly packed, with limited interstitial

space. Tubular basal and adluminal compartments were tightly connected, and germ cells were properly organized, with spermatogonia, spermatocytes, and round spermatids visible at successively higher levels within the epithelium. Leydig cells in the interstitium and Sertoli cells and germ cells within tubules were normal and healthy. However, after SARS-CoV-2 infection, various testicular abnormalities were noted in both the interstitium and seminiferous tubules at 5 and 8 dpi. Interstitial edema of varying severity levels was observed in some areas, either as increased interstitial space between adjacent seminiferous tubules (Fig. 7E, iii at 5 dpi) or with red-stained fluid filling the interstitial space (Fig. 7E, v at 5 dpi). Leydig and Sertoli cells, as well as most germ cells, appeared healthy. However, in some areas within seminiferous tubules, germ cells were severely disorganized, in extreme cases, randomly occupied space throughout the tubule (Fig. 7E, iii, d5). In some areas, the tubules were found to be congested with evidence of prematurely sloughed germ cells in the lumen (Fig. 7E, v at 5 dpi). These results validate our in vitro data and collectively demonstrate that despite no active replication, SARS-CoV-2 infection results in interstitial and tubular abnormalities in the testis of hACE2 mice. These injury markers are similar to what has been observed in humans (7, 60, 61) suggesting that these mice can be used as a model to systematically delineate the indirect effect of SARS-CoV-2 on different aspects of male reproductive health.

Discussion:

Emerging clinical studies highlight that SARS-CoV-2 infection-associated testicular pain, reduced testosterone levels and altered sperm counts are more common in COVID-19 patients than previously thought (5, 7, 8). Further, postmortem studies have

characterized several features of testicular injury including the detachment of SC, apoptosis of undifferentiated spermatogonia, and infiltration of leukocytes in the interstitium. However, the association of these injury markers with virus infection kinetics is not clear. Here, we used different 2D and 3D culture models of primary human testicular cells to show that (i) While SARS-CoV-2 can enter LC and different seminiferous tubular cells, it cannot establish a productive infection in any of these cell types (ii) Inflammatory media from infected airway epithelial cells and plasma from COVID-19 can trigger inflammatory cytokines production and cytotoxicity in testicular cells (iii) Exposure of testicular cells to SARS-CoV-2 E protein increases expression of inflammatory cytokines and induce severe cytotoxicity that is dependent on TLR2 and (iv) intranasal inoculation of K18-hACE2 mice depicted leads to testicular damage in the absence of any replicating virus, thus overall supporting the fact that testicular damage is a bystander effect of SARS-CoV-2 infection.

Susceptibility to SARS-CoV-2 infection is highly cell type-specific and dependent on the presence of entry receptors like ACE2 and serine protease, TMPRSS2 (41). While robust infection of lung alveolar type II epithelial cells is linked to high ACE2 expression, the absence of this receptor and serine proteases is the main reason for the human macrophages, natural killer (NK) cells, dendritic cells, and vascular endothelial cells not being susceptible to SARS-CoV-2 (26, 62). Enterocytes in the gastrointestinal (GI) tract that express very high levels of ACE2 and TMPRSS2 are susceptible to SARS-CoV-2, but the virions produced are very low compared to alveolar type II cells (63, 64) suggesting that just the presence of receptors alone is not enough to establish

458 productive viral infection. Although several groups, including ours, have reported high
459 levels of ACE2 and TMPRSS2 in the human testes including LC, SC, and
460 undifferentiated spermatogonia (26, 28), direct evidence of infection of human testicular
461 cells is lacking. The presence of SARS-CoV-2 RNA in the human postmortem testes
462 tissue is not a common observation and is limited to RT-PCR detection of very low
463 levels of viral genome copies (7). Even in the animal models, subgenomic SARS-CoV-
464 2 RNA was detected only in the intratesticular inoculated hamsters (65). Further, the
465 suggestion that SARS-CoV-2 can infect testes of the rhesus macaques by Madden and
466 colleagues was based on the staining of Spike protein (66) and does not confirm if testis
467 can support active replication of the virus. Therefore, taken together, our data showing
468 the total absence of SARS-CoV-2 virions in the media and no cell death in infected
469 cells, provide direct evidence that SARS-CoV-2 cannot establish productive replication
470 in different testicular cells in vitro. Since virus replication is directly associated with
471 robust inflammatory response, the absence of the induction of the key cytokines in
472 infected cells again supports our notion that none of our in vitro testicular cell models
473 supported virus replication. We speculate this can be either due to the absence of co-
474 localization of TMPRSS2 and ACE2 in the same cell type or the lack of specific host
475 components required for virus replication.
476
477 However, robust data now exists suggesting that COVID-19 leads to severe testicular
478 injury and affects testis function (7). In the absence of active virus replication, tissue
479 injury can be mediated by cytokines storm or exposure to virus proteins (67–69). Mild
480 and severe COVID-19 patients exhibit systemic cytokine profiles similar to other

infectious diseases such as Ebola virus disease (EVD) (70). The elevated levels of TNFα, IL6, IL1, IFNγ, and monocyte chemoattractant protein 1 (MCP1) reported in severe EVD are associated with severe damage to the kidney and vascular system (71). Similarly, dengue nonstructural protein (NS1) shed during acute infection acts as a viral pathogen-associated molecular pattern that activates TLR4 on leukocytes and endothelial cells leading to inflammation and endothelial dysfunction (52). Therefore, we next focused on addressing our alternative hypothesis that testicular injury results from the bystander effect of systemic cytokines. The key cytokines induced by SARS-CoV-2 infected HAE cells support findings from previous studies (72, 73). Our observation of the comparable levels of cytokines in HAE media and COVID-19 plasma is encouraging and supports the notion that inflammatory HAE supernatant can be used to study bystander effects of SARS-CoV-2 associated cytokine storm. Transmigration of SARS-CoV-2 from the apical to the basal side of the inserts has been reported previously, but our data is the first to correlate virus replication with the induction of key inflammatory cytokines in the supernatant of this 2D model. Interestingly, both STC and HTOs exhibited significantly higher cytotoxicity post-exposure to inflammatory media from infected HAE and plasma from COVID-19 patients compared to SC (Fig. 3). Our speculation that this difference is most likely because of the presence of delicate undifferentiated spermatogonia in the STC and HTO was confirmed by the TUNEL assay and agrees with germ cell depletion seen in the testis from COVID-19 patients (6).

While the secretion of E protein by infected cells in COVID-19 patients is not yet determined, two recent studies have shown the presence of SARS-CoV-2 S1 and N proteins in the plasma of 64% of COVID-19 patients in the range of 5-10,000 pg/mL plasma (74). Other studies also report the presence of S1 in the urine and saliva of COVID-19 patients (75) suggesting that the shedding of different SARS-CoV-2 proteins is an outcome of infection and might be an event associated with severe disease. Additionally, the presence of VLPs in different tissues including the testes and the brain is also commonly reported (16, 17). Both S1 and N proteins have been shown to induce inflammation and cell death in macrophages (20, 21), suggesting the potential of these proteins to independently cause cytopathic effects. On the other hand, Zheng and colleagues reported that exposure to S1 did not induce any inflammatory response compared to E in bone marrow-derived macrophages (BMDMs) (76). Therefore, although it was surprising that S1 did not induce any cytopathy in SC and STC, we believe this might be because S1 was not efficiently internalized in these cells (Fig. 6) compared to more phagocytic macrophages. Our data, however, agrees with previous in vitro and in vivo studies that also showed induction of cytokine response, cell death, and lung pathology by SARS-CoV-2 E protein and dependence on the TLR2 pathway (76, 77). There is a consensus view that E, a glycosylated transmembrane protein with ion channel activity, plays an important role not only in viral replication and virion assembly but also in pathogenicity including induction of cytokines and cell death (69). These studies and our data collectively suggest that E protein can trigger an inflammatory response and cause cytopathic effects in the testicular cells independent of SARS-CoV-2 replication.

An important highlight of our study is the validation of the in vitro data in the K18-hACE2 mouse model. Since high expression of hACE2 is mainly in the lungs, as expected very high viral replication was detected in this organ leading to high mouse mortality. Elevated levels of inflammatory cytokines have been reported before not only in the lungs but also in the plasma of these mice (78). Therefore, we believe that the K18-hACE2 mouse model is an appropriate model for studying the bystander effect of SARS-CoV-2 infection. Our data provide the first evidence that the testicular pathological events similar to what is reported in postmortem testis tissue from COVID-19 patients (7) manifest in the K18 hACE2 mice. Seminiferous tubule disorganization, germ cell sloughing, and germ cell apoptosis that we observed in mouse testis sections are well-characterized hallmarks of testicular injury thus establishing K18-hACE2 mice as a tool that would allow to systematically delineate underlying mechanisms at the molecular level in future studies.

Although gross alterations in male reproductive health including lower testosterone levels and decreased sperm count have been well established, our understanding of the mechanisms of SARS-CoV-2 infection-associated testis injury is limited. Few studies have reported presence of viral antigens and/or VLPs in the testis by immunostaining, based on which it has been proposed that testicular injury is the result of direct SARS-CoV-2 infection (79, 80). However, our data present direct evidence that despite the expression of ACE2, human testicular cells do not support productive infection of SARS-CoV-2. Our study also greatly improves our understanding of the indirect effect of virus infection on testicular injury. Collective data suggest that during peak infection, exposure of testicular cells to both cytokine storm and viral antigens may trigger pathological

549 pathways and apoptotic death of germ cells that may be responsible for orchitis symptoms
550 and lower sperm counts reported in COVID-19 patients. However, further investigations
551 are warranted to characterize the testicular injury's short- and long-term effects on fertility
552 markers like testosterone levels, and the specific pathways associated with pathological
553 events. Finally, our findings presented herein suggest the need for long-term follow-up of
554 male reproductive health markers in moderate to severe male COVID-19 patients
555 following recovery.
556
557 **Acknowledgements**
558 This work was partially supported by grants R21AI129465 (SV), R21AI140248 (SV),
559 Victoria S. And Bradley L. Geist Foundation **(**MDT and SV), George F. Straub Trust &
560 Robert C. Perry Fund **(**MDT and SV), and NIH HD072380 and HD106936 (MAW). We
561 thank Ms. Mallory Wilson for technical help with tissue culture and RT-PCR experiments.
562
563 **Figure legends**
564 **Figure 1. Lack of SARS-CoV-2 does not establish a productive infection in human**
565 **testicular cells.** (**A)** Primary SC, LC, STC and HTO were infected with SARS-CoV-2 at
566 MOI 1 and intracellular virus levels were determined at 24, 48 and 96 hrs post-infection
567 (hpi) using qRT-PCR. **(B)** SARS-CoV-2 titers in the supernatant from infected Vero E6,
568 SC, LC, STC and HTO at MOI 1 were measured using plaque assay. **(C)**
569 Representative images of SARS-CoV-2 (MOI 1) infected SC, LC and Vero E6 cells
570 stained for SARS-CoV-2 using anti-Spike (green) at 48 hpi. **(D)** SARS-CoV-2 progeny
571 titers measured by plaque assay in the supernatant from infected SC and LC pre-

572 incubated with 5µg/mL of exogenous serine protease. **(E)** The mRNA fold change of
573 *TNFA, IL6,* and *IFNB1* measured in infected SC, LC, and HTO (MOI 1) using qRT-PCR
574 at 48 hpi. The error bars represent the ±SEM of at least 4 independent infections.
575
576 **Figure 2. Human airway epithelial cells are highly permissive to SARS-CoV-2**
577 **infection and produce inflammatory cytokines. (A)** Fully differentiated primary HAE
578 grown on inserts were infected with SARS-CoV-2 (MOI 1) and infectious virions
579 released on the apical and basal side were quantified using plaque assay **(B)** SARS-
580 CoV-2 RNA measured in HAE at days (D) 1, 2, 4 and 8 post-infection using qRT-PCR
581 **(C)** The transepithelial electrical resistance (TEER) was used to measure the integrity of
582 the air-liquid barrier of HAE inserts at different days post-infection (MOI 1), and
583 expressed in Ohm*cm^2 (Ωcm^2). **(D)** The mRNA fold-change of *TNFA, IL6, IFIT1* and
584 *IFNB1* genes was measured in infected HAE at MOI 1 using qRT-PCR. Error bars
585 represent ±SEM of at least 3 independent infections. **p<0.01; ****p<0.0001.
586
587 **Figure 3. Bystander effect of SARS-CoV-2 on different testicular cells. (A-C)** IL6,
588 IL1β and TNFα levels were measured by ELISA in the mock and UV-inactivated
589 supernatant from infected HAE cells (Inf) (4 dpi), and control (healthy donor) and
590 COVID-19 plasma. **(D)** Percent cell viability assessed in STC at 24 hrs following
591 exposure to UV-inactivated HAE infected (Inf Sup) or control supernatant (Mock Sup),
592 **(E)** Percent viability of STC and HTO exposed to control (Cont) or COVID-19 plasma for
593 24 hrs post-exposure calculated by comparing to corresponding untreated cells **(F)**
594 Viability of SC exposed to UV inactivated HAE infected (Inf Sup) or control (Mock Sup)

595 supernatant at 24hrs post-exposure. (**G)** The fold-change of *IL6, IL1B, TNFA,* and *BAX*
596 transcripts in HTO exposed to control and COVID-19 plasma was measured using qRT-
597 PCR (error bar represents ±SEM of 4 data points and each data point is a pool of RNA
598 from 10 HTO). **(H)** The effect of exposure of HAE supernatant on the mRNA expression
599 of *IL6, IL1B, TNFA* and *BAX* in SC was determined by RT-PCR. Error bars represent
600 ±SEM of at least 3 independent exposures. *p<0.05; **p<0.01; ***p<0.001;
601 ****p<0.0001
602
603 **Figure 4. SARS-CoV-2 infection-derived factors promote apoptotic cell death of**
604 **undifferentiated spermatogonia. (A)** Representative TUNEL staining in STC exposed
605 to supernatant from mock (HAE Sup-Mock) and infected HAE cells (HAE Sup-Inf), and
606 to control and COVID-19 plasma for 24 hrs. The green fluorescence depicts TUNEL+
607 cells. **(B)** Quantification of percent TUNEL positive cells and mean fluorescence
608 intensity in each group. Data represents the average of at least six fields per coverslip
609 from 3 independent experiments captured using Image J. Error bars represent ±SEM.
610 **(C)** STC exposed to UV-inactivated HAE supernatant and COVID-19 plasma were co-
611 stained with TUNEL and UCHL1, a marker for undifferentiated spermatogonia including
612 spermatogonia stem cells (SSC). Co-localization was evaluated by merging TUNEL and
613 UCHL1 and white arrows indicate overlapping green and red staining (yellow).
614 ***p<0.001; ****p<0.0001
615
616 **Figure 5. SARS-CoV-2 Envelope protein triggers cell death and inflammation via**
617 **TLR2**. **(A)** SC cell viability was assessed 24 hrs after exposure to recombinant SARS-

618 CoV-2 spike subunit 1 (S1), nucleocapsid (N) and envelope (E) proteins at 0.25, 0.5, 1
619 and 4ng/µL media in 96-well plates. Exposure of E protein was also conducted in the
620 presence of proteinase K enzyme **(B)** STC were exposed to S1 and E protein at 1 and
621 4ng/µL media and the percent change in cell viability was calculated after 24 hrs. **(C)**
622 Percent change in the cell viability of HTO was evaluated 24 hrs after exposure to
623 recombinant SARS-CoV-2 E and S1 at 4ng. **(D-F)** TNFα, IL6 and IL1β levels in the
624 supernatant STC were measured using ELISA after exposure to recombinant E and S1
625 proteins. **(G)** mRNA fold change of *IL6, IL1B, TNFA* and *BAX* in STC exposed to 4ng/µL
626 of E and S1 proteins was measured at 24 hrs post-exposure using qRT-PCR. **(H)** SC
627 were treated with E protein (4ng) in the presence or absence of TLR2 and TLR4
628 neutralizing antibodies and percent cell viability was measured after 24 hrs of exposure.
629 Error bars represent an average of at least 3-5 independent exposures (±SEM).
630 **p<0.01; ***p<0.001; ****p<0.0001.
631
632 **Figure 6. The uptake of SARS-CoV-2 envelope protein disrupts the morphology of**
633 **the seminiferous tubule cells.** STC were exposed to green fluorophore-conjugated E
634 and S1 proteins (4ng) and the uptake was evaluated after 24 hrs by detecting
635 intracellular virus antigens (green) following staining with DAPI and Phalloidin (red), a
636 marker for actin filaments. **(A)** Representative confocal microscopy image show E
637 protein localization in the cytoplasm (white arrows) and dramatic loss of actin filaments.
638 High-power magnification pictures depict dramatic disruption of the nuclear
639 compartment with genetic material being ejected from the nucleus (blue arrows). **(B)**
640 The mean fluorescence intensity (MFI) of intracellular E and S1 proteins, and **(C)** actin

641 filament length and **(D)** MFI were assessed using Image J in 3 different fields from at
642 least 2 independent experiments. *p<0.05; **p<0.01; ****p<0.0001.
643
644 **Figure 7. SARS-CoV-2 infection in K18-hACE2 mice exhibits severe testicular**
645 **pathology**. **(A)** Eight to twelve weeks old male and female K18-hACE2-transgenic mice
646 were inoculated via the intranasal route with 104 PFU SARS-CoV-2. Survival was
647 monitored for 14 days (n=15). **(B)** Viral RNA in the lung, heart, and testis at days 3, 5,
648 and 8 post-infection (dpi) measured by RT-qPCR. The dotted horizontal line indicates
649 the limit of detection. **(C)** Plaque assay was used to determine SARS-CoV-2 titers in the
650 lung, heart, and testis tissue homogenates. **(D)** Fold change in the gene expression of
651 inflammatory genes *IL6* and *TNFA* was determined in the lung and testis homogenates
652 using qRT-PCR (two independent experiments; n = 4-6 males per time point). **(E)** PAS-
653 staining of testis sections from K18-hACE2 mice following mock (i-ii) or SARS-CoV-2
654 infection at 5 (iii, v) and 8 (iv) dpi. Images show seminiferous tubules from control mice
655 with normal tubular morphology and healthy Leydig (black arrows) and Sertoli cells
656 (white arrows). Insets show healthy round and elongated spermatids typical of the
657 stage. In sections from SARS-CoV-2 infected mice noted abnormalities were interstitial
658 edema (IE) (iii and vi), lack of lumen and overall cell disorganization (iii), separation of
659 germ cell layers from the basal membrane (iv), sloughing of healthy and apoptotic germ
660 cells into the lumen (v, arrowhead and inset). Insets, 3x magnification. Scale, 100 µm.
661
662
663
664

References

1. Sanyaolu A, Okorie C, Marinkovic A, Patidar R, Younis K, Desai P, Hosein Z, Padda I, Mangat J, Altaf M. 2020. Comorbidity and its Impact on Patients with COVID-19. SN Compr Clin Med 2:1069–1076.

2. Tenforde MW, Self WH, Adams K, Gaglani M, Ginde AA, McNeal T, Ghamande S, Douin DJ, Talbot HK, Casey JD, Mohr NM, Zepeski A, Shapiro NI, Gibbs KW, Files DC, Hager DN, Shehu A, Prekker ME, Erickson HL, Exline MC, Gong MN, Mohamed A, Henning DJ, Steingrub JS, Peltan ID, Brown SM, Martin ET, Monto AS, Khan A, Hough CL, Busse LW, ten Lohuis CC, Duggal A, Wilson JG, Gordon AJ, Qadir N, Chang SY, Mallow C, Rivas C, Babcock HM, Kwon JH, Halasa N, Chappell JD, Lauring AS, Grijalva CG, Rice TW, Jones ID, Stubblefield WB, Baughman A, Womack KN, Rhoads JP, Lindsell CJ, Hart KW, Zhu Y, Olson SM, Kobayashi M, Verani JR, Patel MM, Influenza and Other Viruses in the Acutely Ill (IVY) Network. 2021. Association Between mRNA Vaccination and COVID-19 Hospitalization and Disease Severity. JAMA 326:2043–2054.

3. Chen J, Qi T, Liu L, Ling Y, Qian Z, Li T, Li F, Xu Q, Zhang Y, Xu S, Song Z, Zeng Y, Shen Y, Shi Y, Zhu T, Lu H. 2020. Clinical progression of patients with COVID-19 in Shanghai, China. J Infect 80:e1–e6.

4. Mokhtari T, Hassani F, Ghaffari N, Ebrahimi B, Yarahmadi A, Hassanzadeh G. 2020. COVID-19 and multiorgan failure: A narrative review on potential mechanisms. J Mol Histol 51:613–628.

687 5. Griffith DM, Sharma G, Holliday CS, Enyia OK, Valliere M, Semlow AR, Stewart EC,
688 Blumenthal RS. 2020. Men and COVID-19: A Biopsychosocial Approach to
689 Understanding Sex Differences in Mortality and Recommendations for Practice
690 and Policy Interventions. Prev Chronic Dis 17:E63.

691 6. He Y, Wang J, Ren J, Zhao Y, Chen J, Chen X. 2021. Effect of COVID-19 on Male
692 Reproductive System – A Systematic Review. Frontiers in Endocrinology 12.

693 7. Ma X, Guan C, Chen R, Wang Y, Feng S, Wang R, Qu G, Zhao S, Wang F, Wang
694 X, Zhang D, Liu L, Liao A, Yuan S. 2021. Pathological and molecular
695 examinations of postmortem testis biopsies reveal SARS-CoV-2 infection in the
696 testis and spermatogenesis damage in COVID-19 patients. 2. Cell Mol Immunol
697 18:487–489.

698 8. Duarte-Neto AN, Teixeira TA, Caldini EG, Kanamura CT, Gomes-Gouvêa MS, Dos
699 Santos ABG, Monteiro RAA, Pinho JRR, Mauad T, da Silva LFF, Saldiva PHN,
700 Dolhnikoff M, Leite KRM, Hallak J. 2022. Testicular pathology in fatal COVID-19:
701 A descriptive autopsy study. Andrology 10:13–23.

702 9. Rastrelli G, Di Stasi V, Inglese F, Beccaria M, Garuti M, Di Costanzo D, Spreafico F,
703 Greco GF, Cervi G, Pecoriello A, Magini A, Todisco T, Cipriani S, Maseroli E,
704 Corona G, Salonia A, Lenzi A, Maggi M, De Donno G, Vignozzi L. 2021. Low
705 testosterone levels predict clinical adverse outcomes in SARS-CoV-2 pneumonia
706 patients. Andrology 9:88–98.

10. Schroeder M, Schaumburg B, Müller Z, Parplys A, Jarczak D, Nierhaus A, Kloetgen A, Schneider B, Peschka M, Stoll F, Bai T, Jacobsen H, Zickler M, Stanelle-Bertram S, Heer G de, Renné T, Meinhardt A, Heeren J, Aberle J, McHardy AC, Schlüter H, Hiller J, Peine S, Kreienbrock L, Klingel K, Kluge S, Gabriel G. 2020. Sex hormone and metabolic dysregulations are associated with critical illness in male Covid-19 patients. medRxiv https://doi.org/10.1101/2020.05.07.20073817.

11. Guo L, Zhao S, Li W, Wang Y, Li L, Jiang S, Ren W, Yuan Q, Zhang F, Kong F, Lei J, Yuan M. 2021. Absence of SARS-CoV-2 in semen of a COVID-19 patient cohort. Andrology 9:42–47.

12. Holtmann N, Edimiris P, Andree M, Doehmen C, Baston-Buest D, Adams O, Kruessel J-S, Bielfeld AP. 2020. Assessment of SARS-CoV-2 in human semen-a cohort study. Fertil Steril 114:233–238.

13. Clinical Characteristics and Results of Semen Tests Among Men With Coronavirus Disease 2019 | Global Health | JAMA Network Open | JAMA Network. https://jamanetwork.com/journals/jamanetworkopen/fullarticle/2765654. Retrieved 19 April 2022.

14. Pesaresi M, Pirani F, Tagliabracci A, Valsecchi M, Procopio AD, Busardò FP, Graciotti L. 2020. SARS-CoV-2 identification in lungs, heart and kidney specimens by transmission and scanning electron microscopy. Eur Rev Med Pharmacol Sci 24:5186–5188.

15. Martin-Cardona A, Lloreta Trull J, Albero-González R, Paraira Beser M, Andújar X, Ruiz-Ramirez P, Tur-Martínez J, Ferrer C, De Marcos Izquierdo JA, Pérez-Madrigal A, Goiburú González L, Espinós Perez J, Esteve M. 2021. SARS-CoV-2 identified by transmission electron microscopy in lymphoproliferative and ischaemic intestinal lesions of COVID-19 patients with acute abdominal pain: two case reports. BMC Gastroenterology 21:334.

16. Paniz-Mondolfi A, Bryce C, Grimes Z, Gordon RE, Reidy J, Lednicky J, Sordillo EM, Fowkes M. 2020. Central nervous system involvement by severe acute respiratory syndrome coronavirus-2 (SARS-CoV-2). Journal of Medical Virology 92:699–702.

17. Plescia CB, David EA, Patra D, Sengupta R, Amiar S, Su Y, Stahelin RV. 2021. SARS-CoV-2 viral budding and entry can be modeled using BSL-2 level virus-like particles. Journal of Biological Chemistry 296:100103.

18. Le Hingrat Q, Visseaux B, Laouenan C, Tubiana S, Bouadma L, Yazdanpanah Y, Duval X, Burdet C, Ichou H, Damond F, Bertine M, Benmalek N, Choquet C, Timsit J-F, Ghosn J, Charpentier C, Descamps D, Houhou-Fidouh N, Diallo A, Le Mestre S, Mercier N, Paul C, Petrov-Sanchez V, Malvy D, Chirouze C, Andrejak C, Dubos F, Rossignol P, Picone O, Bompart F, Gigante T, Gilg M, Rossignol B, Levy-Marchal C, Beluze M, Hulot JS, Bachelet D, Bhavsar K, Bouadma L, Chair A, Couffignal C, Da Silveira C, Debray MP, Descamps D, Duval X, Eloy P, Esposito-Farese M, Ettalhaoui N, Gault N, Ghosn J, Gorenne I, Hoffmann I, Kafif O, Kali S, Khalil A, Laouénan C, Laribi S, Le M, Le Hingrat Q, Lescure F-X, Lucet

JC, Mentré F, Mullaert J, Peiffer-Smadja N, Peytavin G, Roy C, Schneider M, Mohammed NS, Tagherset L, Tardivon C, Tellier MC, Timsit J-F, Trioux T, Tubiana S, Visseaux B, Vanel N, Basmaci R, Angoulvant F, Kaguelidou F, Pages J, Tual C, Veislinger A, Couffin-Cardiergues S, Esperou H, Houas I, Jaafoura S, Papadopoulos A, Coelho A, Diouf A, Hoctin A, Mambert M, Bouscambert M, Gaymard A, Lina B, Rosa-Calatrava M, Terrier O, Benkerrou D, Dorival C, Meziane A, Téoulé F, Guedj J, Le Nagard H, Lingas G, Neant N, Abel L, Desvallée M, Khan C, Deplanque D, Yazdanpanah Y, Behilill S, Enouf V, Mouquet H, Van Der Werf S, Cervantes-Gonzalez M, D'ortenzio E, Puéchal O, Semaille C, Noret M, Etienne M, Levy Y, Wiedemann A, Duval X, Burdet C, Duval X, Lina B, Tubiana S, Van Der Werf S, Abad F, Abry D, Alavoine L, Allain J-S, Amiel-Taieb K, Audoin P, Augustin S, Ayala S, Bansard H, Bertholon F, Boissel N, Botelho-Nevers E, Bouiller K, Bourgeon M, Boutrou M, Brick L, Bruneau L, Caumes E, Chabouis A, Chan Thien E, Chirouze C, Coignard B, Costa Y, Costenoble V, Cour S, Cracowski C, Cracowski J-L, Deplanque D, Dequand S, Desille-Dugast M, Desmarets M, Detoc M, Dewitte M, Djossou F, Ecobichon J-L, Elrezzi E, Faurous W, Fortuna V, Fouchard J, Gantier E, Gautier C, Gerardin P, Gerset S, Gilbert M, Gissot V, Guillemin F, Hartard C, Hazevis B, Hocquet D, Hodaj E, Ilic-Habensus E, A. J, Jeulin H, Kane M, Kasprzyk E, Kikoine J, Laine F, Laviolle B, Lebeaux D, Leclercq A, Ledru E, Lefevre B, Legoas C, Legrand A, Legrand K, Lehacaut J, Lehur C, Lemouche D, Lepiller Q, Lepuil S, Letienne E, Lucarelli A, Lucet J-C, Madeline I, Maillot A, Malapate C, Malvy D, Mandic M, Marty-Quinternet S, Meghadecha M, Mergeay-Fabre M, Mespoulhe P, Meunier A,

772 Migaud M-C, Motiejunaite J, Gay N, Nguyen D, Oubbea S, Pagadoy M, Paris A,
773 Paris C, Payet C, Peiffer-Smadja N, Perez L, Perreau P, Pierrez N, Pistone T,
774 Postolache A, Rasoamanana P, Reminiac C, Rexah J, Roche-Gouanvic E,
775 Rousseau A, Schoemaecker B, Simon S, Soler C, Somers S, Sow K, Tardy B,
776 Terzian Z, Thy M, Tournier A, Tyrode S, Vauchy C, Verdon R, Vernet P, Vignali V,
777 Waucquier N, Burdet C, Do Thi Thu H, Laouénan C, Mentre F, Pauline M,
778 Tubiana S, Dechanet A, Letrou S, Quintin C, Frezouls W, Le Hingrat Q, Houhou
779 N, Damond F, Descamps D, Charpentier C, Visseaux B, Vabret A, Lina B,
780 Bouscambert M, Van Der Werf S, Behillil S, Gaillanne L, Benmalek N, Attia M,
781 Barbet M, Demeret C, Rose T, Petres S, Escriou N, Barbet M, Petres S, Escriou
782 N, Goyard S, Kafif O, Piquard V, Tubiana S, Coignard B, Mailles A, Simondon A,
783 Dreyere M, Morel B, Vesval T, Inserm, Amat K, Ammour D, Aqourras K, Couffin-
784 Cadiergues S, Delmas C, Desan V, Doute J-M, Esperou H, Hendou S, Kouakam
785 C, Le Meut G, Lemestre S, Leturque N, Marcoul E, Nguefang S, Roufai L, Laurent
786 A, Caillat-Zucman S. 2021. Detection of SARS-CoV-2 N-antigen in blood during
787 acute COVID-19 provides a sensitive new marker and new testing alternatives.
788 Clinical Microbiology and Infection 27:789.e1-789.e5.

789 19. Wang X, Lam J-Y, Wong W-M, Yuen C-K, Cai J-P, Au SW-N, Chan JF-W, To
790 KKW, Kok K-H, Yuen K-Y. 2020. Accurate Diagnosis of COVID-19 by a Novel
791 Immunogenic Secreted SARS-CoV-2 orf8 Protein. mBio 11:e02431-20.

792 20. Barhoumi T, Alghanem B, Shaibah H, Mansour FA, Alamri HS, Akiel MA, Alroqi F,
793 Boudjelal M. 2021. SARS-CoV-2 Coronavirus Spike Protein-Induced Apoptosis,
794 Inflammatory, and Oxidative Stress Responses in THP-1-Like-Macrophages:

795 Potential Role of Angiotensin-Converting Enzyme Inhibitor (Perindopril). Frontiers
796 in Immunology 12.

797 21. Karwaciak I, Sałkowska A, Karaś K, Dastych J, Ratajewski M. 2021. Nucleocapsid
798 and Spike Proteins of the Coronavirus SARS-CoV-2 Induce IL6 in Monocytes and
799 Macrophages-Potential Implications for Cytokine Storm Syndrome. Vaccines
800 (Basel) 9:54.

801 22. Xia B, Shen X, He Y, Pan X, Liu F-L, Wang Y, Yang F, Fang S, Wu Y, Duan Z, Zuo
802 X, Xie Z, Jiang X, Xu L, Chi H, Li S, Meng Q, Zhou H, Zhou Y, Cheng X, Xin X, Jin
803 L, Zhang H-L, Yu D-D, Li M-H, Feng X-L, Chen J, Jiang H, Xiao G, Zheng Y-T,
804 Zhang L-K, Shen J, Li J, Gao Z. 2021. SARS-CoV-2 envelope protein causes
805 acute respiratory distress syndrome (ARDS)-like pathological damages and
806 constitutes an antiviral target. 8. Cell Res 31:847–860.

807 23. Ragab D, Salah Eldin H, Taeimah M, Khattab R, Salem R. 2020. The COVID-19
808 Cytokine Storm; What We Know So Far. Frontiers in Immunology 11.

809 24. Leung PS, Sernia C. 2003. The renin-angiotensin system and male reproduction:
810 new functions for old hormones. J Mol Endocrinol 30:263–270.

811 25. Pan P-P, Zhan Q-T, Le F, Zheng Y-M, Jin F. 2013. Angiotensin-converting
812 enzymes play a dominant role in fertility. Int J Mol Sci 14:21071–21086.

813 26. Zhao Y, Zhao Z, Wang Y, Zhou Y, Ma Y, Zuo W. 2020. Single-Cell RNA
814 Expression Profiling of ACE2, the Receptor of SARS-CoV-2. Am J Respir Crit
815 Care Med 202:756–759.

816 27. Liu X, Chen Y, Tang W, Zhang L, Chen W, Yan Z, Yuan P, Yang M, Kong S, Yan
817 L, Qiao J. 2020. Single-cell transcriptome analysis of the novel coronavirus
818 (SARS-CoV-2) associated gene ACE2 expression in normal and non-obstructive
819 azoospermia (NOA) human male testes. Sci China Life Sci 63:1006–1015.

820 28. Wang Z, Xu X. 2020. scRNA-seq Profiling of Human Testes Reveals the Presence
821 of the ACE2 Receptor, A Target for SARS-CoV-2 Infection in Spermatogonia,
822 Leydig and Sertoli Cells. 4. Cells 9:920.

823 29. Strange DP, Jiyarom B, Pourhabibi Zarandi N, Xie X, Baker C, Sadri-Ardekani H,
824 Shi P-Y, Verma S. 2019. Axl Promotes Zika Virus Entry and Modulates the
825 Antiviral State of Human Sertoli Cells. mBio 10:e01372-19.

826 30. Pendergraft SS, Sadri-Ardekani H, Atala A, Bishop CE. 2017. Three-dimensional
827 testicular organoid: a novel tool for the study of human spermatogenesis and
828 gonadotoxicity in vitro. Biol Reprod 96:720–732.

829 31. Strange DP, Zarandi NP, Trivedi G, Atala A, Bishop CE, Sadri-Ardekani H, Verma
830 S. 2018. Human testicular organoid system as a novel tool to study Zika virus
831 pathogenesis. Emerg Microbes Infect 7:82.

832 32. Sadri-Ardekani H, Mizrak SC, van Daalen SKM, Korver CM, Roepers-Gajadien HL,
833 Koruji M, Hovingh S, de Reijke TM, de la Rosette JJMCH, van der Veen F, de
834 Rooij DG, Repping S, van Pelt AMM. 2009. Propagation of human spermatogonial
835 stem cells in vitro. JAMA 302:2127–2134.

836 33. Kumar M, Roe K, Orillo B, Muruve DA, Nerurkar VR, Gale M, Verma S. 2013.
837 Inflammasome adaptor protein Apoptosis-associated speck-like protein containing
838 CARD (ASC) is critical for the immune response and survival in west Nile virus
839 encephalitis. J Virol 87:3655–3667.

840 34. Etievant S, Bal A, Escuret V, Brengel-Pesce K, Bouscambert M, Cheynet V,
841 Generenaz L, Oriol G, Destras G, Billaud G, Josset L, Frobert E, Morfin F,
842 Gaymard A. 2020. Performance Assessment of SARS-CoV-2 PCR Assays
843 Developed by WHO Referral Laboratories. J Clin Med 9:1871.

844 35. Mulay A, Konda B, Garcia G, Yao C, Beil S, Sen C, Purkayastha A, Kolls JK,
845 Pociask DA, Pessina P, de Aja JS, Garcia-de-Alba C, Kim CF, Gomperts B,
846 Arumugaswami V, Stripp BR. 2020. SARS-CoV-2 infection of primary human lung
847 epithelium for COVID-19 modeling and drug discovery. bioRxiv
848 2020.06.29.174623.

849 36. Strange DP, Jiyarom B, Sadri-Ardekani H, Cazares LH, Kenny TA, Ward MD,
850 Verma S. 2021. Paracrine IFN Response Limits ZIKV Infection in Human Sertoli
851 Cells. Frontiers in Microbiology 12.

852 37. Kumar M, Verma S, Nerurkar VR. 2010. Pro-inflammatory cytokines derived from
853 West Nile virus (WNV)-infected SK-N-SH cells mediate neuroinflammatory
854 markers and neuronal death. J Neuroinflammation 7:73.

855 38. Maison DP, Nerurkar VR. 2021. Research Methodology to Define the Introduction
856 of the SARS-CoV-2 B.1.429 Variant in Hawaii. Res Sq rs.3.rs-378702.

857 39. Kumar M, Roe K, Nerurkar PV, Namekar M, Orillo B, Verma S, Nerurkar VR. 2012.
858 Impaired virus clearance, compromised immune response and increased mortality
859 in type 2 diabetic mice infected with West Nile virus. PLoS One 7:e44682.

860 40. Verma S, Saksena S, Sadri-Ardekani H. 2020. ACE2 receptor expression in testes:
861 implications in coronavirus disease 2019 pathogenesis†. Biology of Reproduction
862 103:449–451.

863 41. Hoffmann M, Kleine-Weber H, Schroeder S, Krüger N, Herrler T, Erichsen S,
864 Schiergens TS, Herrler G, Wu N-H, Nitsche A, Müller MA, Drosten C, Pöhlmann
865 S. 2020. SARS-CoV-2 Cell Entry Depends on ACE2 and TMPRSS2 and Is
866 Blocked by a Clinically Proven Protease Inhibitor. Cell 181:271-280.e8.

867 42. Kim Y, Jang G, Lee D, Kim N, Seon JW, Kim Y, Lee C. 2022. Trypsin enhances
868 SARS-CoV-2 infection by facilitating viral entry. Arch Virol 167:441–458.

869 43. Fajgenbaum DC, June CH. 2020. Cytokine Storm. New England Journal of
870 Medicine 383:2255–2273.

871 44. Ahmadian E, Hosseiniyan Khatibi SM, Razi Soofiyani S, Abediazar S, Shoja MM,
872 Ardalan M, Zununi Vahed S. 2020. Covid-19 and kidney injury: Pathophysiology
873 and molecular mechanisms. Rev Med Virol e2176.

874 45. Legrand M, Bell S, Forni L, Joannidis M, Koyner JL, Liu K, Cantaluppi V. 2021.
875 Pathophysiology of COVID-19-associated acute kidney injury. 11. Nat Rev
876 Nephrol 17:751–764.

877 46. Tang N, Li D, Wang X, Sun Z. 2020. Abnormal coagulation parameters are
878 associated with poor prognosis in patients with novel coronavirus pneumonia. J
879 Thromb Haemost 18:844–847.

880 47. Geng Y-J, Wei Z-Y, Qian H-Y, Huang J, Lodato R, Castriotta RJ. 2020.
881 Pathophysiological characteristics and therapeutic approaches for pulmonary
882 injury and cardiovascular complications of coronavirus disease 2019. Cardiovasc
883 Pathol 47:107228.

884 48. Cardiovascular Implications of Fatal Outcomes of Patients With Coronavirus
885 Disease 2019 (COVID-19) | Cardiology | JAMA Cardiology | JAMA Network.
886 https://jamanetwork.com/journals/jamacardiology/fullarticle/2763845. Retrieved 7
887 February 2022.

888 49. Pensato U, Muccioli L, Cani I, Janigro D, Zinzani PL, Guarino M, Cortelli P, Bisulli
889 F. 2021. Brain dysfunction in COVID-19 and CAR-T therapy: cytokine storm-
890 associated encephalopathy. Ann Clin Transl Neurol 8:968–979.

891 50. Frontiers | Ebola Virus Glycoprotein Induces an Innate Immune Response In vivo
892 via TLR4 | Microbiology.
893 https://www.frontiersin.org/articles/10.3389/fmicb.2017.01571/full. Retrieved 11
894 February 2022.

895 51. Shed GP of Ebola Virus Triggers Immune Activation and Increased Vascular
896 Permeability.

897 https://journals.plos.org/plospathogens/article?id=10.1371/journal.ppat.1004509.
898 Retrieved 11 February 2022.

899 52. Modhiran N, Watterson D, Muller DA, Panetta AK, Sester DP, Liu L, Hume DA,
900 Stacey KJ, Young PR. 2015. Dengue virus NS1 protein activates cells via Toll-like
901 receptor 4 and disrupts endothelial cell monolayer integrity. Sci Transl Med
902 7:304ra142.

903 53. Chen J, Ng MM-L, Chu JJH. 2015. Activation of TLR2 and TLR6 by Dengue NS1
904 Protein and Its Implications in the Immunopathogenesis of Dengue Virus Infection.
905 PLOS Pathogens 11:e1005053.

906 54. McCray PB, Pewe L, Wohlford-Lenane C, Hickey M, Manzel L, Shi L, Netland J, Jia
907 HP, Halabi C, Sigmund CD, Meyerholz DK, Kirby P, Look DC, Perlman S. 2007.
908 Lethal infection of K18-hACE2 mice infected with severe acute respiratory
909 syndrome coronavirus. J Virol 81:813–821.

910 55. Oladunni FS, Park J-G, Pino PA, Gonzalez O, Akhter A, Allué-Guardia A, Olmo-
911 Fontánez A, Gautam S, Garcia-Vilanova A, Ye C, Chiem K, Headley C, Dwivedi
912 V, Parodi LM, Alfson KJ, Staples HM, Schami A, Garcia JI, Whigham A, Platt RN,
913 Gazi M, Martinez J, Chuba C, Earley S, Rodriguez OH, Mdaki SD, Kavelish KN,
914 Escalona R, Hallam CRA, Christie C, Patterson JL, Anderson TJC, Carrion R,
915 Dick EJ, Hall-Ursone S, Schlesinger LS, Alvarez X, Kaushal D, Giavedoni LD,
916 Turner J, Martinez-Sobrido L, Torrelles JB. 2020. Lethality of SARS-CoV-2
917 infection in K18 human angiotensin-converting enzyme 2 transgenic mice. 1. Nat
918 Commun 11:6122.

919 56. Moreau GB, Burgess SL, Sturek JM, Donlan AN, Petri WA, Mann BJ. 2020.
920 Evaluation of K18-hACE2 Mice as a Model of SARS-CoV-2 Infection. Am J Trop
921 Med Hyg 103:1215–1219.

922 57. Arce VM, Costoya JA. 2021. SARS-CoV-2 infection in K18-ACE2 transgenic mice
923 replicates human pulmonary disease in COVID-19. 3. Cell Mol Immunol 18:513–
924 514.

925 58. Oladunni FS, Park J-G, Pino PA, Gonzalez O, Akhter A, Allué-Guardia A, Olmo-
926 Fontánez A, Gautam S, Garcia-Vilanova A, Ye C, Chiem K, Headley C, Dwivedi
927 V, Parodi LM, Alfson KJ, Staples HM, Schami A, Garcia JI, Whigham A, Platt RN,
928 Gazi M, Martinez J, Chuba C, Earley S, Rodriguez OH, Mdaki SD, Kavelish KN,
929 Escalona R, Hallam CRA, Christie C, Patterson JL, Anderson TJC, Carrion R,
930 Dick EJ, Hall-Ursone S, Schlesinger LS, Alvarez X, Kaushal D, Giavedoni LD,
931 Turner J, Martinez-Sobrido L, Torrelles JB. 2020. Lethality of SARS-CoV-2
932 infection in K18 human angiotensin-converting enzyme 2 transgenic mice. 1. Nat
933 Commun 11:6122.

934 59. Winkler ES, Bailey AL, Kafai NM, Nair S, McCune BT, Yu J, Fox JM, Chen RE,
935 Earnest JT, Keeler SP, Ritter JH, Kang L-I, Dort S, Robichaud A, Head R,
936 Holtzman MJ, Diamond MS. 2020. SARS-CoV-2 infection of human ACE2-
937 transgenic mice causes severe lung inflammation and impaired function. 11. Nat
938 Immunol 21:1327–1335.

939 60. Yang M, Chen S, Huang B, Zhong J-M, Su H, Chen Y-J, Cao Q, Ma L, He J, Li X-
940 F, Li X, Zhou J-J, Fan J, Luo D-J, Chang X-N, Arkun K, Zhou M, Nie X. 2020.

941 Pathological Findings in the Testes of COVID-19 Patients: Clinical Implications.
942 Eur Urol Focus 6:1124–1129.

943 61. Duarte-Neto AN, Teixeira TA, Caldini EG, Kanamura CT, Gomes-Gouvêa MS, Dos
944 Santos ABG, Monteiro RAA, Pinho JRR, Mauad T, da Silva LFF, Saldiva PHN,
945 Dolhnikoff M, Leite KRM, Hallak J. 2022. Testicular pathology in fatal COVID-19:
946 A descriptive autopsy study. Andrology 10:13–23.

947 62. Schimmel L, Chew KY, Stocks CJ, Yordanov TE, Essebier P, Kulasinghe A,
948 Monkman J, dos Santos Miggiolaro AFR, Cooper C, de Noronha L, Schroder K,
949 Lagendijk AK, Labzin LI, Short KR, Gordon EJ. 2021. Endothelial cells are not
950 productively infected by SARS-CoV-2. Clinical & Translational Immunology
951 10:e1350.

952 63. Diao B, Wang C, Wang R, Feng Z, Zhang J, Yang H, Tan Y, Wang H, Wang C, Liu
953 L, Liu Y, Liu Y, Wang G, Yuan Z, Hou X, Ren L, Wu Y, Chen Y. 2021. Human
954 kidney is a target for novel severe acute respiratory syndrome coronavirus 2
955 infection. 1. Nat Commun 12:2506.

956 64. Monteil V, Kwon H, Prado P, Hagelkrüys A, Wimmer RA, Stahl M, Leopoldi A,
957 Garreta E, Hurtado Del Pozo C, Prosper F, Romero JP, Wirnsberger G, Zhang H,
958 Slutsky AS, Conder R, Montserrat N, Mirazimi A, Penninger JM. 2020. Inhibition
959 of SARS-CoV-2 Infections in Engineered Human Tissues Using Clinical-Grade
960 Soluble Human ACE2. Cell 181:905-913.e7.

961 65. Li C, Ye Z, Zhang AJ-X, Chan JF-W, Song W, Liu F, Chen Y, Kwan MY-W, Lee
962 AC-Y, Zhao Y, Wong BH-Y, Yip CC-Y, Cai J-P, Lung DC, Sridhar S, Jin D, Chu H,
963 To KK-W, Yuen K-Y. 2022. Severe acute respiratory syndrome coronavirus 2
964 (SARS-CoV-2) infections by intranasal or testicular inoculation induces testicular
965 damage preventable by vaccination in golden Syrian hamsters. Clinical Infectious
966 Diseases ciac142.

967 66. Madden PJ, Thomas Y, Blair RV, Samer S, Doyle M, Midkiff CC, Doyle-Meyers LA,
968 Becker ME, Arif MS, McRaven MD, Simons LM, Carias AM, Martinelli E, Lorenzo-
969 Redondo R, Hultquist JF, Villinger FJ, Veazey RS, Hope TJ. 2022. An
970 immunoPET probe to SARS-CoV-2 reveals early infection of the male genital tract
971 in rhesus macaques. bioRxiv https://doi.org/10.1101/2022.02.25.481974.

972 67. Ragab D, Salah Eldin H, Taeimah M, Khattab R, Salem R. 2020. The COVID-19
973 Cytokine Storm; What We Know So Far. Frontiers in Immunology 11.

974 68. Khan S, Shafiei MS, Longoria C, Schoggins JW, Savani RC, Zaki H. 2021. SARS-
975 CoV-2 spike protein induces inflammation via TLR2-dependent activation of the
976 NF-κB pathway. eLife 10:e68563.

977 69. Xia B, Shen X, He Y, Pan X, Liu F-L, Wang Y, Yang F, Fang S, Wu Y, Duan Z, Zuo
978 X, Xie Z, Jiang X, Xu L, Chi H, Li S, Meng Q, Zhou H, Zhou Y, Cheng X, Xin X, Jin
979 L, Zhang H-L, Yu D-D, Li M-H, Feng X-L, Chen J, Jiang H, Xiao G, Zheng Y-T,
980 Zhang L-K, Shen J, Li J, Gao Z. 2021. SARS-CoV-2 envelope protein causes
981 acute respiratory distress syndrome (ARDS)-like pathological damages and
982 constitutes an antiviral target. 8. Cell Res 31:847–860.

983 70. Chousterman BG, Swirski FK, Weber GF. 2017. Cytokine storm and sepsis
984 disease pathogenesis. Semin Immunopathol 39:517–528.

985 71. Reynard S, Journeaux A, Gloaguen E, Schaeffer J, Varet H, Pietrosemoli N, Mateo
986 M, Baillet N, Laouenan C, Raoul H, Mullaert J, Baize S. 2019. Immune
987 parameters and outcomes during Ebola virus disease. JCI Insight 4:125106.

988 72. Vanderheiden A, Ralfs P, Chirkova T, Upadhyay AA, Zimmerman MG, Bedoya S,
989 Aoued H, Tharp GM, Pellegrini KL, Manfredi C, Sorscher E, Mainou B, Lobby JL,
990 Kohlmeier JE, Lowen AC, Shi P-Y, Menachery VD, Anderson LJ, Grakoui A,
991 Bosinger SE, Suthar MS. 2020. Type I and Type III Interferons Restrict SARS-
992 CoV-2 Infection of Human Airway Epithelial Cultures. Journal of Virology
993 94:e00985-20.

994 73. Ryu G, Shin H-W. 2021. SARS-CoV-2 Infection of Airway Epithelial Cells. Immune
995 Netw 21:e3.

996 74. Ogata AF, Maley AM, Wu C, Gilboa T, Norman M, Lazarovits R, Mao C-P, Newton
997 G, Chang M, Nguyen K, Kamkaew M, Zhu Q, Gibson TE, Ryan ET, Charles RC,
998 Marasco WA, Walt DR. 2020. Ultra-Sensitive Serial Profiling of SARS-CoV-2
999 Antigens and Antibodies in Plasma to Understand Disease Progression in COVID-
1000 19 Patients with Severe Disease. Clinical Chemistry 66:1562–1572.

1001 75. George S, Pal AC, Gagnon J, Timalsina S, Singh P, Vydyam P, Munshi M, Chiu
1002 JE, Renard I, Harden CA, Ott IM, Watkins AE, Vogels CBF, Lu P, Tokuyama M,
1003 Venkataraman A, Casanovas-Massana A, Wyllie AL, Rao V, Campbell M,

1004 Farhadian SF, Grubaugh ND, Cruz CSD, Ko AI, Perez AZB, Akaho EH, Moledina
1005 DG, Testani J, John AR, Ledizet M, Mamoun CB, Team and the YI. 2021.
1006 Evidence for SARS-CoV-2 Spike Protein in the Urine of COVID-19 Patients.
1007 Kidney360 2:924–936.

1008 76. Zheng M, Karki R, Williams EP, Yang D, Fitzpatrick E, Vogel P, Jonsson CB,
1009 Kanneganti T-D. 2021. TLR2 senses the SARS-CoV-2 envelope protein to
1010 produce inflammatory cytokines. 7. Nat Immunol 22:829–838.

1011 77. Mandala VS, McKay MJ, Shcherbakov AA, Dregni AJ, Kolocouris A, Hong M. 2020.
1012 Structure and drug binding of the SARS-CoV-2 envelope protein transmembrane
1013 domain in lipid bilayers. 12. Nat Struct Mol Biol 27:1202–1208.

1014 78. Yinda CK, Port JR, Bushmaker T, Offei Owusu I, Purushotham JN, Avanzato VA,
1015 Fischer RJ, Schulz JE, Holbrook MG, Hebner MJ, Rosenke R, Thomas T, Marzi
1016 A, Best SM, de Wit E, Shaia C, van Doremalen N, Munster VJ. 2021. K18-hACE2
1017 mice develop respiratory disease resembling severe COVID-19. PLoS Pathog
1018 17:e1009195.

1019 79. 2022. Testes found to viral reservoir for SARS-CoV-2 replication. News-
1020 Medical.net. https://www.news-medical.net/news/20220213/Testes-found-to-viral-
1021 reservoir-for-SARS-CoV-2-replication.aspx. Retrieved 18 April 2022.

1022 80. Costa GMJ, Lacerda SMSN, Figueiredo AFA, Wnuk NT, Brener MRG, Campolina-
1023 Silva GH, Kauffmann-Zeh A, Pacifico LG, Versiani AF, Andrade LM, Antunes MM,
1024 Souza FR, Cassali GD, Caldeira-Brant AL, Chiarini-Garcia H, Costa VV, Fonseca

1025 FG da, Nogueira ML, Campos GRF, Kangussu LM, Martins EMN, Antonio LM,
1026 Bittar C, Rahal P, Aguiar RS, Mendes BP, Procópio MS, Furtado TP, Guimaraes
1027 YL, Menezes GB, Martinez-Marchal A, Brieno-Enriquez M, Orwig KE, Furtado
1028 MH. 2022. SARS-CoV-2 infects, replicates, elevates angiotensin II and activates
1029 immune cells in human testes. medRxiv
1030 https://doi.org/10.1101/2022.02.05.22270327.

1031

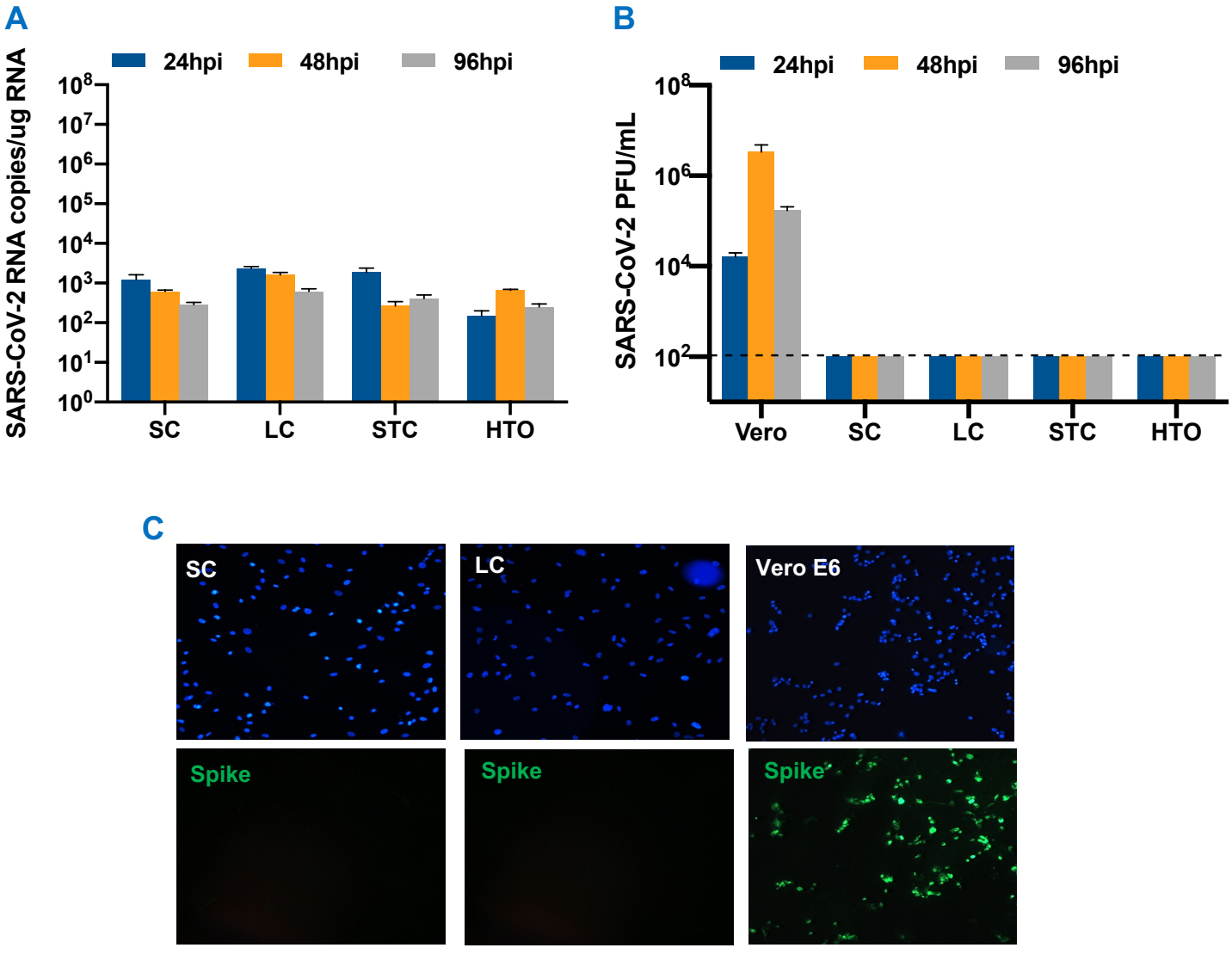

Figure 1

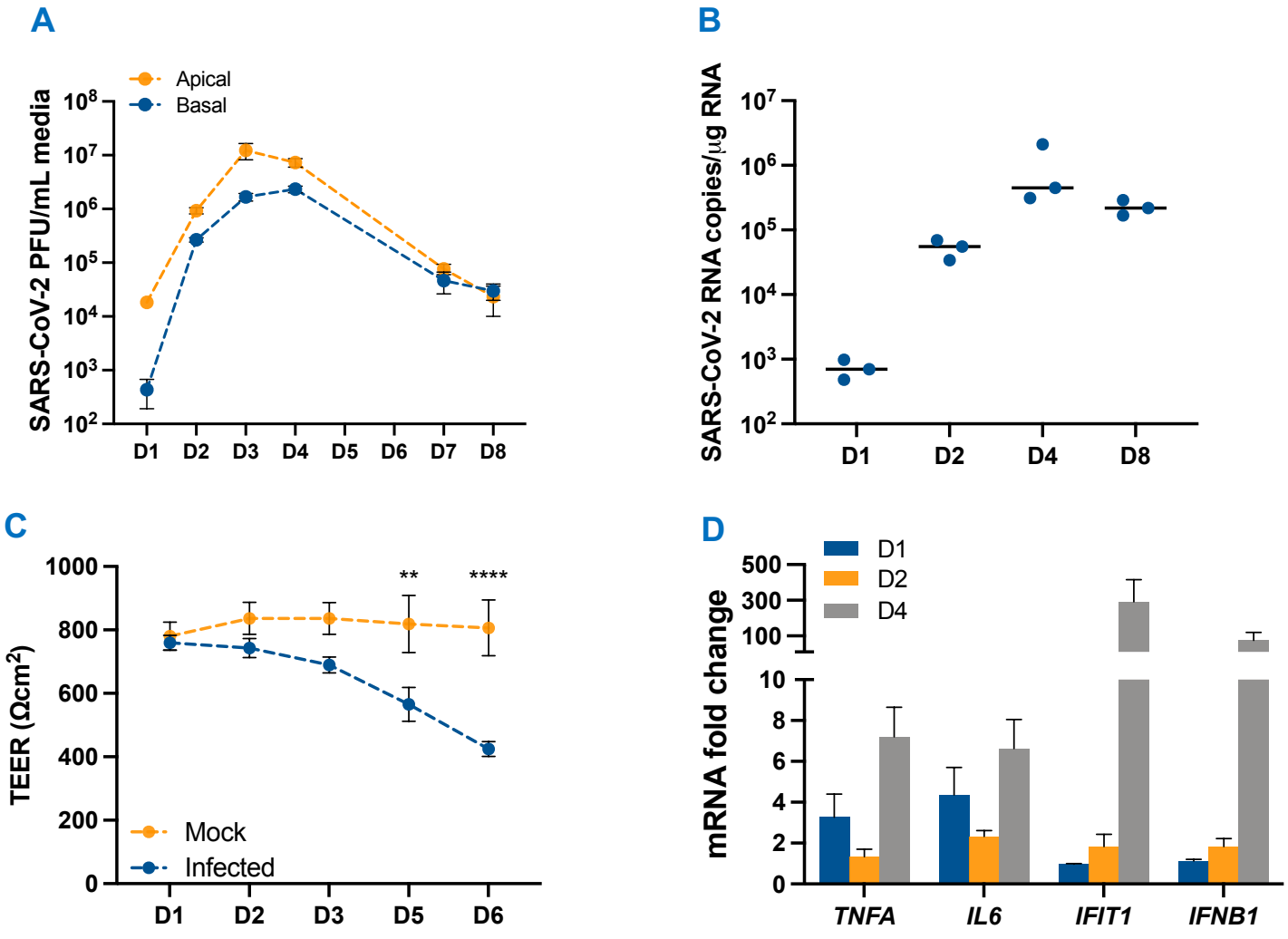

Figure 2

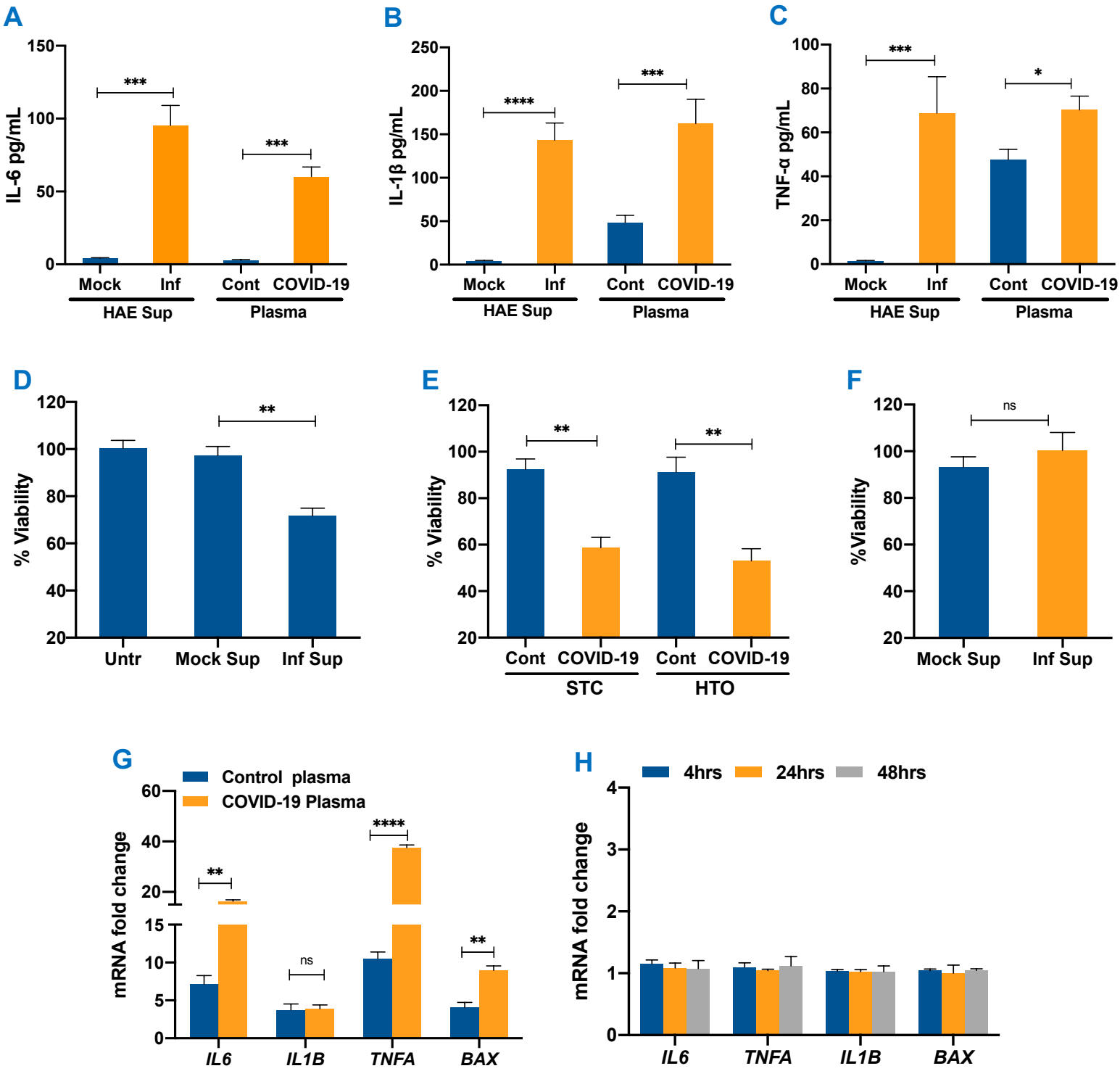

Figure 3

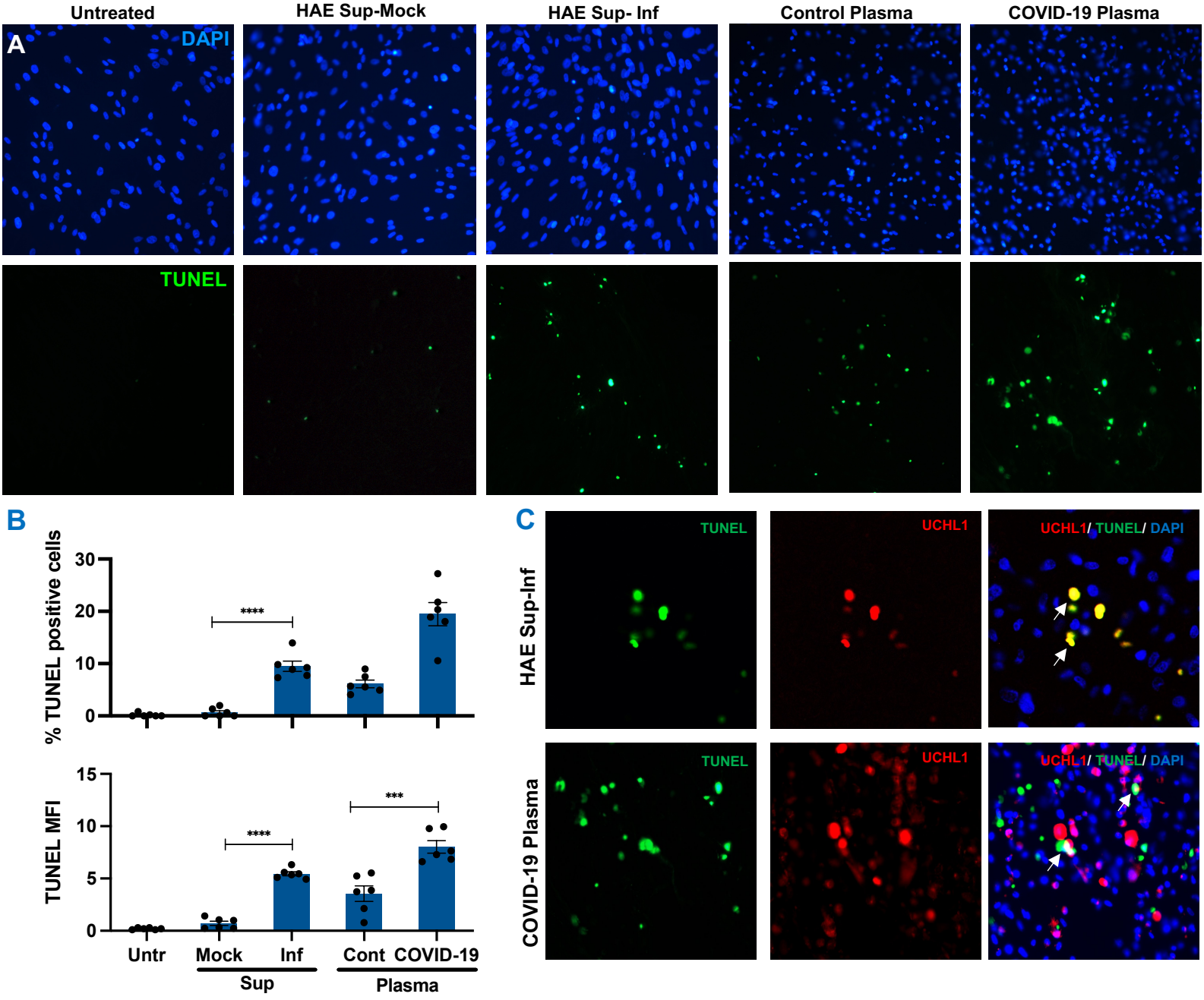

Figure 4

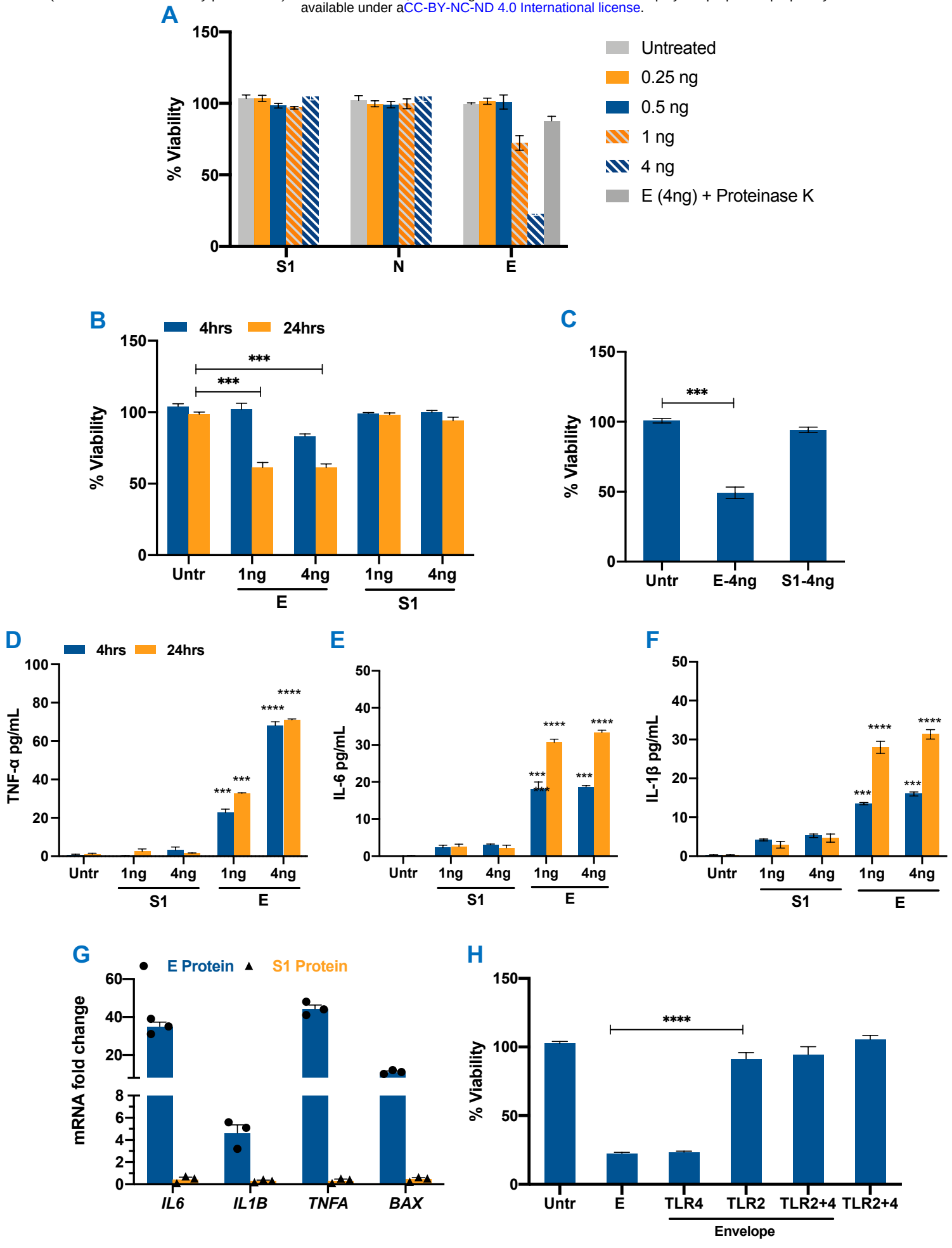

Figure 5

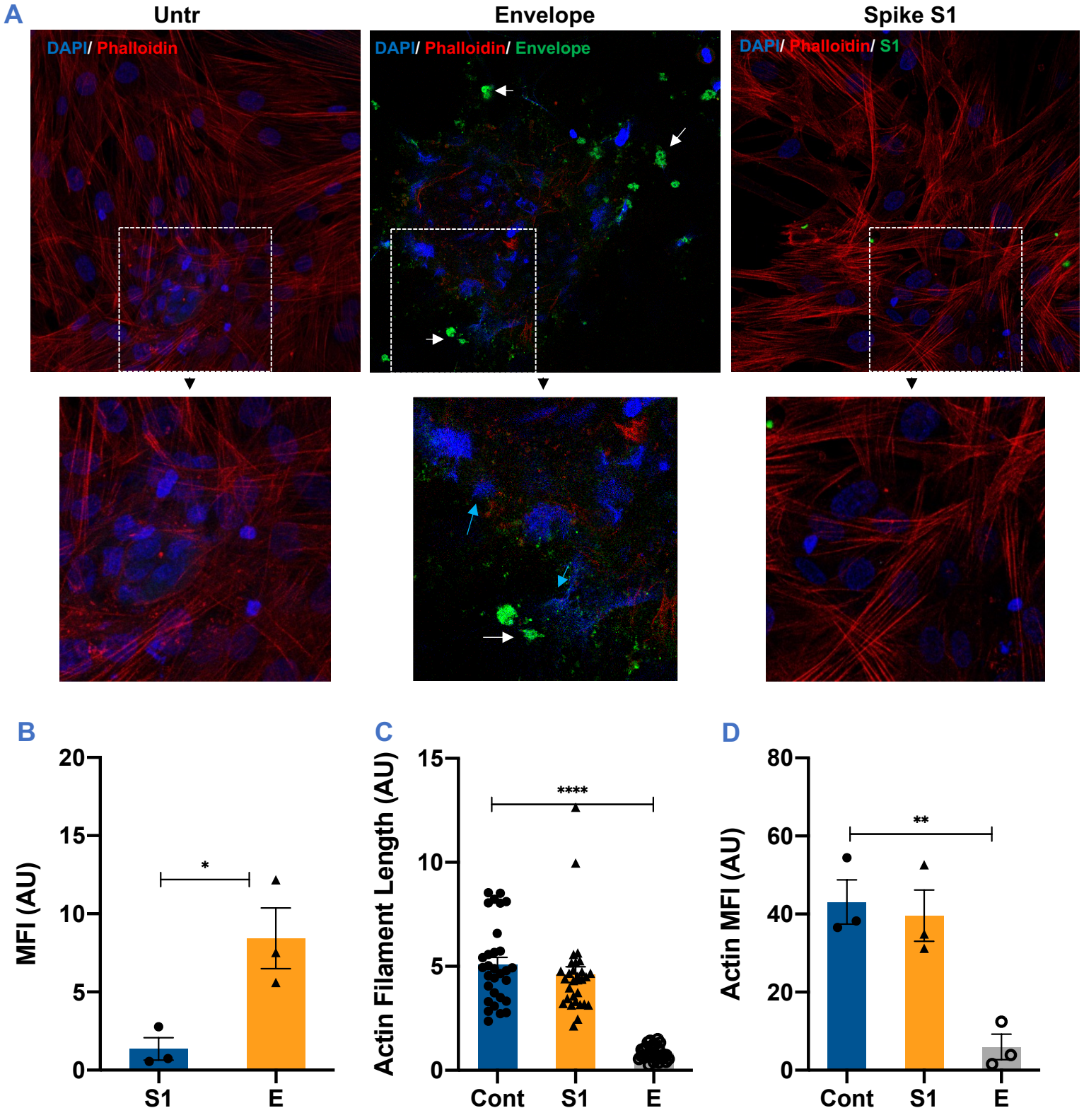
A
Untr
Envelope
Spike S1
DAPI/ Phalloidin
DAPI/ Phalloidin/ Envelope
DAPI/ Phalloidin/ S1
B
MFI (AU)
20
15
10
5
0
*
S1
E
C
Actin Filament Length (AU)
15
10
5
0
****
Cont
S1
E
D
Actin MFI (AU)
80
60
40
20
0
**
Cont
S1
E

Figure 6

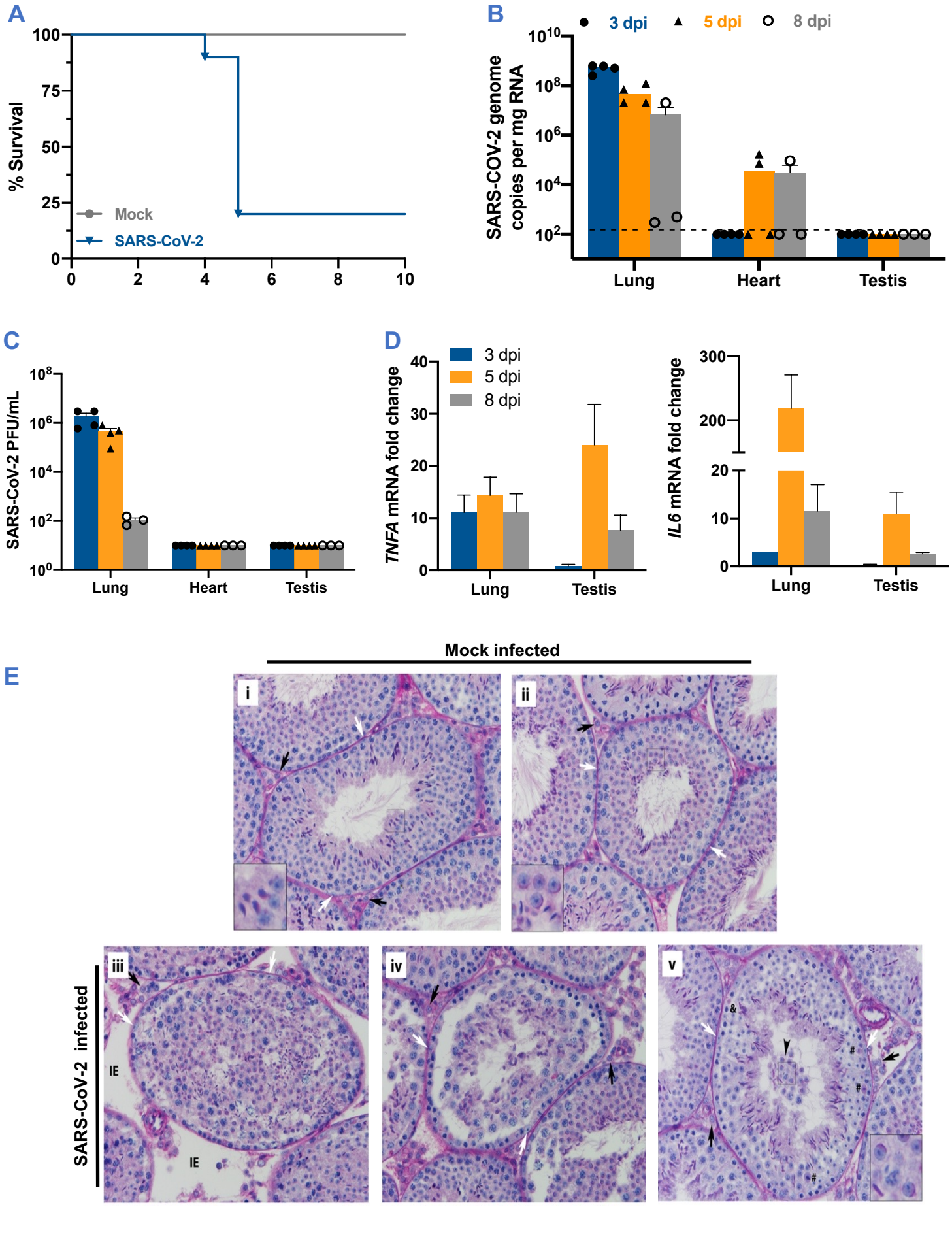
A
% Survival
Mock
SARS-CoV-2
B
3 dpi
5 dpi
8 dpi
SARS-COV-2 genome copies per mg RNA
Lung
Heart
Testis
C
SARS-CoV-2 PFU/mL
Lung
Heart
Testis
D
TNFA mRNA fold change
IL6 mRNA fold change
Lung
Testis
E
Mock infected
SARS-CoV-2 infected
IE

Figure 7